Available online at www.sciencedirect.com
ScienceDirect
Coordination Chemistry Reviews 252 (2008) 1387–1408
COORDINATION CHEMISTRY REVIEWS
www.elsevier.com/locate/ccr

Review

Traversing the coordination chemistry and chemical biology of hydroxamic acids

Rachel Codd *

Discipline of Pharmacology, School of Medical Sciences, University of Sydney, New South Wales 2006, Australia

Received 11 January 2007
Available online 10 August 2007

Contents

Abstract

Hydroxamic acids, $R_C C(O)N(R_N)OH$ (R_C = alkyl/aryl; R_N = alkyl/aryl or H), coordinate a wide variety of transition metal ions predominantly as the monoanionic hydroxamato or dianionic (R_N = H) hydroximato *O*,*O*′-bidentate chelate. Analysis of X-ray crystallographic data from 25 hydroxamato and 17 hydroximato mononuclear non-oxo-containing complexes with bidentate *O*,*O*′-coordination from monohydroxamic acids shows a strong ($R \geq 0.92$) positive correlation between the metal ion radius and the M—OC or M—ON bond lengths; in almost all complexes, M—OC > M—ON. A map of bond lengths in the second coordination sphere (C—N, C—O, N—O), compared to the corresponding bond lengths in free hydroxamic acids, provides insight into the dominant resonance structures of the coordinated ligands. The diverse coordination chemistry of hydroxamic acids is reflected in the groups of complexes which have been characterized by X-ray crystallography: homo- and hetero-metallic complexes of higher nuclearity, metallacrowns, and Pt(II) and Pd(II) complexes, which show non-*O*,*O*′-type coordination modes. The coordination

* Tel.: +61 2 9351 6738; fax: +61 2 9351 3868.
E-mail address: rcodd@med.usyd.edu.au.

0010-8545/$ – see front matter
doi:10.1016/j.ccr.2007.08.001

chemistry of hydroxamic acids is relevant in the context of chemical biology since these bioligands: (i) coordinate metal sites in the Ni(II)-containing metalloprotein, urease, and the Zn(II)-containing metalloproteins, matrix metalloproteases (MMPs), carbonic anhydrase and tumor necrosis factor-α converting enzyme (TACE); and (ii) feature as the Fe(III)-binding functional groups in bacterially derived Fe(III) sequestration molecules called siderophores. Each of (i) and (ii) couples into aspects of human medicine, in terms of hydroxamic acid-based inhibition of MMPs and related enzymes and the treatment of Fe(III) overload disease, which is currently treated using the mesylate salt of desferrioxamine B (DFOB), a linear trihydroxamic acid originally sourced from the soil bacterium, *Streptomyces pilosus*. The X-ray crystal structure of Fe(III)-loaded DFOB (ferrioxamine B: FOB) bound to the iron-siderophore periplasmic transport protein from *Escherichia coli* (FhuD) shows that FOB adopts a chiral and geometric form in the binary FOB–FhuD complex that is distinct from that observed in free FOB.

Keywords: Hydroxamic acids; Hydroxamato/imato coordination complexes; Hydroxamic acids, metalloproteins and drug design

1. Introduction

Hydroxamic acids, R_CC(O)N(R_N)OH (R_C = alkyl/aryl; R_N = alkyl/aryl or H), have a high binding affinity to a range of transition metal ions, particularly Fe(III), and are ligands ubiquitous in coordination chemistry and chemical biology. The dominant coordination mode in metal-hydroxamic acid complexes is the *O*,*O*′-bidentate chelate in which the ligand is either singly deprotonated (hydroxamato) or doubly (R_N = H) deprotonated (hydroximato). The intensely coloured complexes of solutions of hydroxamic acids and metals have been widely used in analytical chemistry applications. Vanadium(V), for example, can be detected to 0.15 ppm upon complexation with *N*-phenylbenzohydroxamic acid (pbhaH) giving a violet solution with $\varepsilon \sim 10^4\ M^{-1}\ cm^{-1}$ [1]. Hydroxamic acids that dominate coordination chemistry and chemical biology are acetohydroxamic acid (ahaH$_2$), benzohydroxamic acid (bhaH$_2$), salicylhydroxamic acid (shiH$_3$) and the linear and cyclic trihydroxamic acids of the desferrixoamine family (DFOB, DFOE), which are derived from *Streptomyces* species. The strong affinity between most transition metal ions and hydroxamic acids is reflected in the magnitudes of the overall stability constant, which for [Fe(bhaH)$_3$] or [Fe(ahaH)$_3$] is $\sim 10^{28}$ [2].

The affinity between the hydroxamic acid group and Fe(III) is exploited in the natural world in the form of one of the classes of siderophores, which are molecules produced by bacteria to solubilize the limited available Fe(III) under oxic and pH neutral conditions. Many excellent review articles [3–7] and book chapters [8–12] are available on siderophores and it is not the intention of this work to review siderophores *per se*. The Fe(III) that is essential for viable bacterial growth, is ultimately made available via cell-surface proteins that specifically recognize the Fe(III)–siderophore complex, transport the complex to the cytoplasm and release the Fe(III)/(II) [13]. Hydroxamic acid-based sequestration of Fe(III) is also a key part of the treatment of transfusional-dependent blood disorders in humans, such as β-thalassemia. Left untreated, the excess Fe(III) that accumulates from frequent blood transfusions can lead to organ failure and death; chelation therapy using the mesylate salt of DFOB, is an essential part of the treatment regime for these patients [14,15].

The affinity between hydroxamic acids and transition metal ions is apparent in the X-ray crystal structures of Ni(II)-containing urease [16] or Zn(II)-containing metalloproteins, such as carbonic anhydrase [17], or matrix metalloproteases (MMPs), where hydroxamic acids are bound to the Ni(II) or Zn(II) active sites [18–22]. The MMPs, enzymes involved in the degradation and remodeling of the extracellular matrix and implicated in carcinogenesis and tumor invasion processes, are of particular interest since the binding of hydroxamic acids to the Zn(II) active site renders these ligands as potential leads for MMP inhibition [23–25]. Given the expansive role that hydroxamic acids play in chemical biology, it is important that up-to-date knowledge of the status of the coordination chemistry of this key class of bioligand is available. This is the central purpose of this review. In the 15 years that have passed since the coordination chemistry of hydroxamic acids was most recently reviewed for this journal [2,26], a wealth of new hydroxamic acid coordination complexes have been characterized.

This review opens with an overview of some of the fundamental chemistry of hydroxamic acids before moving to the central focus of mapping coordination complexes of hydroxamic acids that have been characterized by X-ray crystallography, including complexes formed with transition metals, metalloids and actinides. Complexes discussed in this review include classical mononuclear homoleptic complexes, mononuclear heteroleptic complexes, homometallic di- and trinuclear complexes and a stand-alone class of compounds with polyfunctional hydroxamic acids, called metallacrowns. Hydroxamic acid complexes which exhibit atypical non-*O*,*O*′-bidentate coordination modes and/or coordination isomerism are also described. Bond lengths in the first coordination shell (M–OC, M–ON) for 42 *O*,*O*′-coordinated mononuclear hydroxamato/imato complexes have been extracted from X-ray crystal structure data and are presented as a function of the metal ion radii. The bond lengths in the second coordination shell of selected complexes (C–N, C–O, N–O) are discussed in terms of the dominant resonance forms of the hydroxamato/imato ligands. The scope of this review does not include the coordination chemistry of thiohydroxamic acids or hydroxypyridinone ligands. The review discusses briefly the solution chemistry of metal–hydroxamic acid complexes as a prelude to highlighting the roles that hydroxamic acids play in chemical biology. The X-ray crystal structures of Ni(II)- or Zn(II)-containing metalloproteins with bound hydroxamic acid ligands are discussed. A comparison of the structure of Fe(III)-loaded DFOB (ferrioxamine B: FOB) and of the binary complex formed between FOB and the iron–siderophore periplasmic transport protein from *Escherichia coli* (FhuD) is described before closing the review with a brief discussion of the clinical use of DFOB in humans and some future perspectives of

hydroxamic acids. With the backdrop of siderophores as inspiration, this review ultimately aims to thread together recent advances in the coordination chemistry and chemical biology of hydroxamic acids, one of the staring functional groups of siderophores.

2. Hydroxamic acids

2.1. Synthesis

Hydroxamic acids (**1**) are produced from the reaction between a carboxylic acid derivative and hydroxylamine (R_N = H) or an *N*-alkyl/aryl hydroxylamine. Most often, the carboxylic acid is converted to the ester, acid chloride or acid anhydride prior to reaction with the hydroxylamine nucleophile (Scheme 1) [27–31]. More recent methods for the synthesis of hydroxamic acids include the conversion of *N*-acyloxazolidinones using samarium triflate as a Lewis acid [32] and the use of peptide synthetic methods, such as the use of coupling reagents (cyanuric chloride, thiouronium salts) for the conjugation of carboxylic acids or *N*-protected amino acids and hydroxylamine [33,34] or the use of *N*-linked hydroxylamine solid supports [35]. Hydroxamic acids have also been synthesized in high yield and purity using a modified Angeli-Rimini reaction between an aldehyde and solid-supported *N*-hydroxybenzenesulfonamide [36].

Reverse or retro-hydroxamic acids are *N*-alkyl/arylated derivatives of *N*-formylhydroxylamine (**1**: R_C = H, R_N = alkyl, aryl); the retro-hydroxamic acid of $ahaH_2$ (**1**: R_C = Me, R_N = H), for example, is *N*-methyl-*N*-formylhydroxylamine ($CH_3N(OH)CH(O)$). The *O*-benzylation of the *N*-formyl- or *N*-acetylhydroxylamine group is common in solution-based syntheses of retro-hydroxamic acids [37,38]. More recently, retro-hydroxamic acids have been prepared via sold-phase synthesis from Wang-*O*-hydroxylamine resin subject to formylation and *N*-alkylation reactions [39].

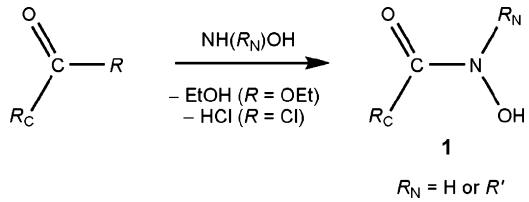

Scheme 1. Synthesis of hydroxamic acids.

2.2. Acid–base properties and structure

Hydroxamic acids are weak acids with pK_a values of the N–OH proton in aqueous solvents of the order 8.5–9.4 [40]. In non-protic solvents, such as dimethylsulfoxide (DMSO), studies have shown that select hydroxamic acids, including benzohydroxamic acid ($bhaH_2$; **1**: R_C = Ph, R_N = H) act as N–H acids, rather than as N–OH acids [41,42]. Partial *N*-deprotonation of $ahaH_2$ has been proposed from recent near edge X-ray absorption fine structure (NEXAFS) spectroscopic data [43]. Primary hydroxamic acids (R_N = H) can undergo two successive deprotonation events (Scheme 2): loss of the first proton yields the hydroxamate anion (**2a**, **2b**); loss of the second proton yields the hydroximate dianion (**3a**, **3b**). The hydroxamic acid, hydroxamate and hydroximate groups can exhibit *cis*/*trans* (or *Z*, *E*) isomerism (**1a**, **1b**) resulting from the free rotation about the C–N bond, keto (R_CC(O)NHR_N)-iminol (R_CC(OH)NR_N) tautomerism (**1b**, **1c**) and have several resonance contributing structures (**2a**, **2b** and **3a**, **3b**). The relative stabilities of these hydroxamic acid structures and of metal–hydroxamato/imato complexes have been studied using density functional theory [44–48].

One of the most widely studied hydroxamic acids, $ahaH_2$, has a pK_a value of 9.28 [40]. *N*-Methylacetohydroxamic acid (**1**: R_C = R_N = Me) is a stronger acid (pK_a = 8.80) than $ahaH_2$, which at first pass appears to be counterintuitive, since it would be expected that the electron donating effect of the

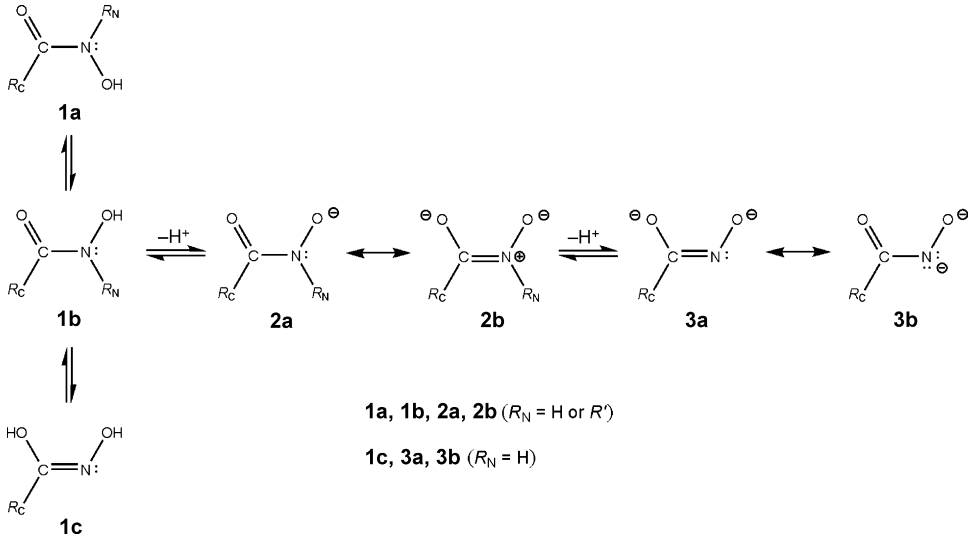

Scheme 2. Structures of hydroxamic acids (**1**), hydroxamates (**2**) and hydroximates (**3**) with representations of *cis–trans* isomerism (**1a**, **1b**), tautomerism (**1b**, **1c**) and resonance (**2a**, **2b**; **3a**, **3b**).

Table 1
Geometry and selected bond lengths of hydroxamic acids characterized by X-ray crystallography

Ligand	Abbreviation	Geometry	Bond length (Å)			Reference
			C═O	C─N	N─O	
Acetohydroxamic acid	$ahaH_2$	*cis*-	1.235	1.320	1.394	[49]
Benzohydroxamic acid	$bhaH_2$	*cis*-	1.240	1.324	1.389	[62,63]
Salicylhydroxamic acid	$shiH_3$	*cis*-	1.258	1.315	1.390	[64]
N-(3-Cyanophenyl)acetohydroxamic acid	*m*-cpahaH	*trans*-	1.240	1.352	1.405	[52]
N-(4-Cyanophenyl)acetohydroxamic acid	*p*-cpahaH	*trans*-	1.227	1.365	1.394	[51]
N-Phenyl-2-methoxybenzohydroxamic acid	pmbhaH	*cis*-	1.237	1.333	1.394	[65]
N-(4-Methylphenyl)acetohydroxamic acid	mpahaH	*trans*-	1.239	1.356	1.400	[53]
N-Methyl-4-methylbenzohydroxamic acid	mmbhaH	*trans*-	1.244	1.339	1.405	[53]

N-substituted methyl group would destabilize the conjugate base (**2a**) relative to the conjugate base of $ahaH_2$, where $R_N = H$. The weaker acidity of $ahaH_2$, compared to the *N*-substituted acetohydroxamic acids, can be rationalized in the context of hydrogen bonding. The X-ray crystal structure of $ahaH_2 \cdot 0.5H_2O$ reveals the presence of a network of intermolecular hydrogen bonding involving the N–H donor group (molecule 1) and the CO acceptor group (molecule 2) in addition to hydrogen bonding interactions between $ahaH_2$ and water [49]. Since a less extensive hydrogen-bonding network would be accessible for *N*-substituted hydroxamic acids ($R_N \neq H$), deprotonation of the N–OH group would be driven to a greater extent compared to the unsubstituted ($R_N = H$) analogues. *N*-Phenylacetohydroxamic acid (**1**: $R_C = Me$, $R_N = Ph$) is a stronger acid than *N*-methylacetohydroxamic acid (pK_a values of 8.51 and 8.80, respectively), since the electron-withdrawing *N*-phenyl group will stabilize the conjugate base (**2a**) to a larger extent than the *N*-methyl homologue.

The X-ray crystal structure of $ahaH_2 \cdot 0.5H_2O$ [49] and of the simplest hydroxamic acid, formylhydroxamic acid (formylhydroxylamine; **1**: $R_C = R_N = H$) [50] show the molecules adopt in the solid state the *cis*- (or *Z*) configuration (**1b**); most other *C*- and *N*-substituted hydroxamic acids, such as *N*-(4-cyanophenyl)acetohydroxamic acid [51], *N*-(3-cyanophenyl)acetohydroxamic acid [52] and the isomers, *N*-methyl-4-methylbenzohydroxamic acid (*N*-methyl-4-toluylohydroxamic acid) and *N*-(4-methylphenyl)acetohydroxamic acid [53], adopt the *trans*- (or *E*) configuration (**1a**) due to steric effects. In the gas phase, the *Z*-amide conformer (**1b**) is found to be the most stable, both as the neutral (**1b**) and singly deprotonated species (**2b**) [54]. The solution equilibrium between the *E* and *Z* conformers of hydroxamic acids has been studied by NMR spectroscopy [55–58]; for *N*-methyl-substituted hydroxamic acids, the *Z*/*E* ratio increases with the bulk of the R_C substituent in DMSO-d_6, $CDCl_3$ or C_6D_6 [59]. While as free ligands, X-ray crystallography reveals a *trans*-geometry of many (but not all) *C*- and *N*-substituted hydroxamic acids (Table 1), there is a change to a *cis*-geometry that must occur upon metal ion coordination. Studies have shown that the nature of the *C*- and *N*-substituents influence the stability of the metal–hydroxamato/imato complex [60,61], whereby, a more stable complex is formed when both the *C*- and *N*-substituents are electron donating, thereby increasing the localized negative charge on the coordinating oxygen atoms (**2a**, **2b**, **3a**, **3b**).

2.3. Biosynthesis

In this age of chemical biology, it is instructive to consider how hydroxamic acids are synthesized in Nature. The linear (B, G_1) or cyclic (E; nocardamine) series of desferrioxamines (trihydroxamic acids) can be deconstructed to condensation products of dicarboxylic acids (succinic acid) and diamines (1,5-pentanediamine) with *N*-hydroxylation of every second amide group.

The genome sequence of the hydroxamic acid-utilizing bacterium, *Streptomyces coelicolor*, has been completed [67], which, taken together with results of previous studies, has led to the identification of the gene cluster that directs desferrioxamine E (DFOE) biosynthesis in this organism [66,68]. The first step in the biosynthesis of DFOE (Scheme 3) is the decarboxylation of L-lysine (**4**) by the enzyme, DesA, to give cadaverine (**5**). The enzyme, DesB, which has high sequence homology to FAD-dependent amine monoxygenases, catalyses the *N*-hydroxylation reaction to give *N*-hydroxycadaverine (**6**). DesC catalyses the *N*-acylation of *N*-hydroxycadaverine to give 4-[(5-aminopentyl)hydroxyamino]-4-oxo-butanoic acid (**7**). Oligomerisation of three subunits of **7** followed by cyclisation (all catalysed by DesD) results in the formation of DFOE (**8**). The total synthesis of DFOE [69], retro-DFOE and retro-DFOG [70], retro-ferrichrome [71] and several other complex hydroxamic acid-based siderophores have been reported, such as alcaligin [72], bisucaberin [73], aerobactin [74] and more recently, danoxamine [75] and desferrisalmycin B [76].

3. Coordination chemistry of hydroxamic acids

3.1. Touring the Periodic Table

Coordination complexes of metals or metalloids with hydroxamic acids are spread widely throughout the Periodic Table (Fig. 1) with many characterized by X-ray crystallography (Tables 2 and 3). This subsection gives a snapshot of the breadth of the coordination chemistry of hydroxamic acids; further details of the complexes are given in subsequent sections (Sections 3.2–3.6). Mononuclear homoleptic complexes with

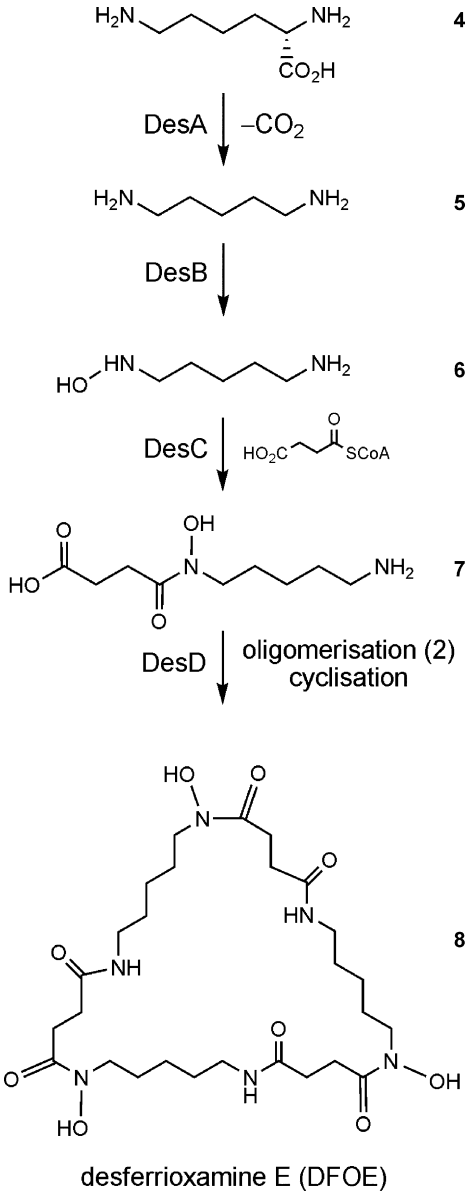

Scheme 3. Biosynthesis of DFOE, as adapted from Ref [66].

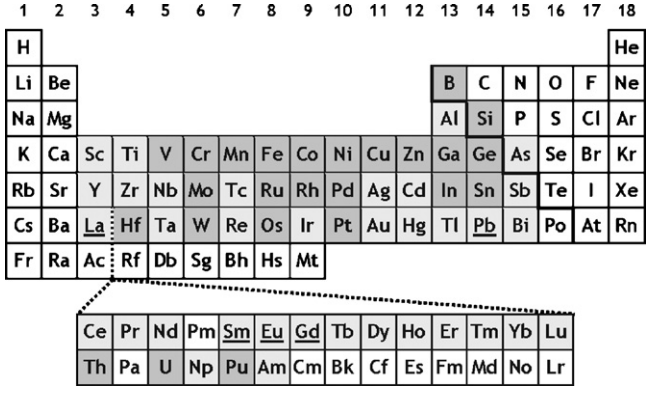

Fig. 1. Homometallic hydroxamic acid complexes (Groups 3–15) characterized by X-ray crystallography (dark shade) or in solution (light shade). Central metals in heterometallic–polyfunctional hydroxamic acid complexes (metallacrowns) characterized by X-ray crystallography are underlined.

Table 2
Selected average bond lengths (Å) in mononuclear homoleptic complexes with bidentate *O*,*O*′-hydroxamato/imato coordination from monohydroxamic acids

Complex[a]	Average bond length (Å)					Reference
	C—O	C—N	N—O	M—ON	M—OC	
$[B(bha)_2]^-$	1.331	1.267	1.421	1.467	1.473	[82]
fac-$[Si(aha)_3]^{2-}$	1.326	1.279	1.430	1.762	1.787	[85]
fac-$[Si(bha)_3]^{2-}$	1.321	1.294	1.427	1.782	1.780	[85]
mer-$[Si(bha)_3]^{2-}$	1.325	1.293	1.429	1.775	1.782	[85]
fac-$[Cr(bhaH)_3]$	1.273	1.305	1.373	1.960	1.985	[86]
fac-$[Cr(bha)_3]^{3-}$	1.304	1.307	1.441	1.955	1.969	[83]
mer-$[Cr(bha)_3]^{3-}$	1.317	1.295	1.420	1.955	1.987	[83]
$[Fe(bhaH)_3]$	1.278	1.303	1.370	1.980	2.058	[78]
$[Fe(mpaha)_3]$	1.268	1.324	1.384	1.970	2.054	[87]
$[Fe(p\text{-}cpaha)_3]$	1.271	1.328	1.385	1.952	2.055	[51]
$[Fe(mmbha)_3]$	1.277	1.315	1.377	1.983	2.045	[87]
fac-$[Fe(ahaH)_3]$	1.268	1.295	1.378	1.971	2.056	[78]
mer-$[Fe(ahaH)_3]$	1.270	1.299	1.369	1.980	2.044	[78]
mer-$[Co(bha)_3]^{3-}$	1.317	1.293	1.413	1.884	1.907	[84]
$[Cu(mmmbha)_2]$[b]	1.283	1.307	1.381	1.882	1.935	[88]
fac-$[Ga(bhaH)_3]$	1.268	1.308	1.377	1.952	1.996	[89]
$[Ga(mmbha)_3]$	1.278	1.312	1.378	1.952	1.988	[87]
fac-$[Ge(bha)_3]^{2-}$	1.322	1.293	1.424	1.885	1.885	[85]
mer-$[In(bhaH)_3]$	1.270	1.299	1.370	2.141	2.164	[90]
$[Hf(pbha)_4]$[c]	1.267	1.325	1.375	2.114	2.258	[91]
$[Th(ipdmbha)_4]$[d]	1.261	1.308	1.370	2.359	2.464	[92]

[a] Ligand abbreviations as given in Table 1 unless otherwise indicated.
[b] mmmbhaH = *N*-methyl-(3-methoxy-4-methyl)benzohydroxamic acid.
[c] pbhaH = *N*-phenylbenzohydroxamic acid.
[d] ipdmbhaH = *N*-isopropyl-3,3-dimethylbutanohydroxamic acid.

bidentate *O*,*O*′-hydroxamato/imato coordination from monohydroxamic acids (Table 2) have been characterized with Fe(III), Cr(III), Co(III), Ga(III), In(III), Si(IV) or Ge(IV) (octahedral geometry), Cu(II) (square planar geometry), B(III) (tetrahedral geometry), or Hf(IV) or Th(IV) (distorted dodecahedral geometry). Mononuclear heteroleptic complexes with bidentate *O*,*O*′-hydroxamato/imato coordination from monohydroxamic acids (Table 3) have been characterized with Si(IV), V(V), Co(II), Co(III), Ni(II), Zn(II), Mo(VI), Ru(III), Rh(III), Sn(IV), W(VI), Os(III), Pt(II) and U(IV). Dinuclear μ-(*N*)*O*-bridged-hydroxamato complexes with Ni(II), Co(II), Zn(II) or Mn(II) and $ahaH_2$, $bhaH_2$ or salicylhydroxamic acid (**1**: R_C = 2-hydroxy-Ph, R_N = H) have been characterized by X-ray crystallography in addition to novel Zn(II)-$bhaH_2$ or Co(II)-$ahaH_2$ trinuclear complexes and a heptanuclear Ni(II) complex with 2-(dimethylamino)phenylhydroxamic acid.

Complexes formed between polyfunctional hydroxamic acids, such as $shiH_3$ or α- or β-aminohydroxamic acids, and Mn(III)/(II), Cu(II) or Ni(II) have snowflake-like architectures and fall into a class of compounds known as metallacrowns. Metallacrowns form clusters reminiscent of crown ethers with centrally orientated O atoms which encapsulate a metal ion that can be either the same as ((Cu(II), Ni(II), Mn(III)/(II))) or different from (La(III), Pb(II), Sm(III), Eu(III), Gd(III)) the flanking metal ions. The Group 10 metals (Ni(II), Pt(II), Pd(II)) show diverse non-*O*,*O*′-coordination modes with polyfunctional hydroxamic acids, including, in the case of Pt(II)–$shiH_3$ complexes, coordination isomerism.

Table 3
Selected bond lengths (Å) in mononuclear heteroleptic complexes with bidentate *O*,*O*′-hydroxamato/imato coordination from monohydroxamic acids

Complex[a]	Average bond length (Å)						Reference
	M—L[b]	C—O[c]	C—N	N—O	M—ON	M—OC	
$[(Me_2NH)CH_2Si(aha)_2]$	N/A	1.330_{av}	1.284_{av}	1.443_{av}	1.688_{av}	1.767_{av}	[105]
$[(Me_2NH)CH_2Si(bha)_2]$	N/A	1.334_{av}	1.288_{av}	1.435_{av}	1.696_{av}	1.767_{av}	[105]
$[VO(bhaH)_2Cl]$	$1.599_{(O)}$	1.238	1.338	1.347	1.851	2.192	[93]
	$1.599_{(O)}$	1.272_{cis}	1.299	1.378	1.953	2.011	
$[VO(O^iPr)(L(2-))]_2$[d]	1.591	1.210	1.373	1.379	1.883	2.185	[93]
	1.591	1.273_{cis}	1.302	1.373	1.940	2.041	
[VO(OMe)(pthaH)$_2$][e]	1.608	1.255	1.317	1.364	1.900	2.219	[114]
	1.608	1.261_{cis}	1.308	1.378	1.930	2.116	
[VO(pbha)(aabhz)][f,g]	1.584	1.243	1.343	1.375	1.864	2.242	[94]
[VO(shedH)(shiH)][h]	1.602	1.273	1.321	1.379	1.846	2.123	[95]
[VO(pbha)(mmsal)][i]	1.581	1.246	1.328	1.372	1.854	2.181	[96]
trans-[Co(tpa)(aha)]$^+$[j]	N/A	1.305	1.286	1.431	1.858	1.878	[115]
cis-[Co(tpa)(aha)]$^+$[j]	N/A	1.319	1.283	1.418	1.855	1.867	[115]
cis-[Co(tpa)(pha)]$^+$[j,k]	N/A	1.331	1.282	1.429	1.867	1.867	[115]
cis-[Co(tpa)(bha)]$^+$[j]	N/A	1.325	1.296	1.407	1.874	1.856	[115]
[Co(tpa)(mmst)]$^+$[j,l]	N/A	1.330	1.284	1.413	1.870	1.870	[116]
cis-[Co(tpa)(ahaH)]$^{2+}$[j]	N/A	1.292	1.286	1.393	1.870	1.879	[115]
cis-[Co(tpa)(phaH)]$^{2+}$[j,k]	N/A	1.289	1.268	1.390	1.863	1.863	[115]
[Co(6-Ph$_2$tpa)(ahaH)]$^+$[m]	N/A	1.269	1.313	1.379	1.935	2.141	[107]
[Ni([12]aneN$_3$-mc2)(ahaH)]$^+$[n]	N/A	1.260	1.299	1.376	2.002	2.009	[117]
[Ni(6-Ph$_2$tpa)(ahaH)]$^+$[m]	N/A	1.272	1.311	1.384	2.020	1.997	[107]
[Ni(bppa)(ahaH$_2$)]$^{2+}$[o]	N/A	1.251	1.334	1.392	2.091	2.037	[118]
[Zn(6-Ph$_2$tpa)(ahaH)]$^+$[m]	N/A	1.269	1.303	1.382	1.992	2.042	[107]
[Zn(en)(bhaH)$_2$][p]	N/A	1.260	1.315	1.367	2.079	2.142	[63]
[Zn(Tp^{Me,Ph})(ahaH)][q]	N/A	1.256	1.314	1.386	1.976	2.102	[24]
cis-[Mo(O)$_2$(paha)$_2$][r]	1.7033	1.270	1.303	1.392	2.025	2.199	[97]
	1.7026	1.260	1.319	1.387	2.022	2.191	
cis-[Mo(O)$_2$(epaha)$_2$][s]	1.7038	1.264	1.307	1.390	2.010	2.206	[97]
	1.6923	1.263	1.311	1.384	2.024	2.195	
cis-[Mo(O)$_2$(phxha)$_2$][t]	1.725	1.233	1.382	1.387	1.998	2.163	[98]
	1.651	1.254	1.310	1.350	2.019	2.191	
cis-[Mo(O)$_2$(glyhaH)$_2$][u]	1.723	1.307	1.275	1.424	2.001	2.140	[99]
	1.706	1.285	1.293	1.426	1.982	2.145	
cis-[Mo(O)$_2$(ahaH)(*aha*)]$^-$ (A)[v]	1.717	1.286	1.287	1.410	1.953	2.110	[100]
cis-[Mo(O)$_2$(*ahaH*)(aha)]$^-$ (A)[v]	1.712	1.268	1.297	1.364	2.014	2.224	
cis-[Mo(O)$_2$(ahaH)(*aha*)]$^-$ (B)[v]	1.719	1.291	1.289	1.415	1.953	2.108	[100]
cis-[Mo(O)$_2$(*ahaH*)(aha)]$^-$ (B)[v]	1.714	1.265	1.300	1.365	2.008	2.229	
[MoO(L″(1−))(bha)(*bhaH*)][w]	1.685	1.286	1.330	1.369	2.047	2.172	[101]
[MoO(L″(1−))(*bha*)(bhaH)][w]	1.685	1.324_{cis}	1.297	1.419	1.990	1.995	
cis-[Mo(O)$_2$(bha)$_2$]$^{2-}$[y] (A)[v]	1.750	1.330	1.386	1.388	1.988	2.117	[101]
	1.733	1.307	1.354	1.432	1.996	2.162	
cis-[Mo(O)$_2$(bha)$_2$]$^{2-}$[y] (B)[v]	1.731	1.294	1.250	1.414	1.952	2.139	[101]
	1.704	1.281	1.187	1.450	1.989	2.181	
[Ru(edtaH$_2$)(ombhaH)][x]	N/A	1.323	1.319	1.368	1.964	2.019	[108]
[Rh(pbha)$_2$Cl(PPh$_3$)][g]	2.326	1.297	1.309	1.373	2.017	2.013	[102]
	2.326	1.274_{cis}	1.324	1.386	2.002	2.113	
$[(CH_3)_2Sn(mbhaH)_2]$[y]	N/A	1.259	1.319	1.376	2.089	2.449	[103]
$[(Ph)_3Sn(pbha)]$[g]	N/A	1.26	1.30	1.38	2.09	2.31	[119]
cis-[W(O)$_2$(bhaH)$_2$]	1.705	1.253	1.317	1.353	1.985	2.167	[104]
	1.690	1.276	1.292	1.388	1.974	2.127	
[Os(tfaha)(tfa)(NO)(PPh$_3$)$_2$][z]	N/A	1.310	1.277	1.421	1.973	2.069	[110]
[Pt(shiH)(PPh$_3$)$_2$]	N/A	1.322	1.297	1.398	2.045	2.072	[120]
[Pt(bha)(DMSO)$_2$]	N/A	1.326	1.288	1.406	1.960	2.013	[121]

Table 3 (*Continued*)

Complex[a]	Average bond length (Å)						Reference
	M—L[b]	C—O[c]	C—N	N—O	M—ON	M—OC	
[Pt(shiH)(DMSO)$_2$]	N/A	1.324	1.283	1.422	1.982	1.990	[121]
trans-[U(O)$_2$(MeOH)(pbha)$_2$][g]	2.367$_{(MeOH)}$	1.267	1.321	1.389	2.418	2.405	[106]
	2.367$_{(MeOH)}$	1.338$_{cis}$	1.283	1.331	2.379	2.346	

[a] Ligand abbreviations as given in Table 1 unless otherwise indicated.
[b] L = O^{2-}, Cl^-, MeOH.
[c] Unless otherwise indicated, in bis-chelate hydroxamato/imato complexes, each chelate is defined separately whereby the CO group is *trans* to the M—L bond specified.
[d] O^{i}Pr = isopropoxy; L(2−) = *N*,*N*′-dihydroxy-*N*,*N*′-diisopropylheptanediamido.
[e] pthaH$_2$ = *p*-toluylohydoxamic acid.
[f] aabhzH$_2$ = acetylacetone benzoylhydrazonao-*O*,*N*,*O*′.
[g] pbhaH = *N*-phenylbenzohydroxamic acid.
[h] shedH$_2$ = *N*-(salicylideneaminato)-*N*′-(2-hydroxyethyl)ethylenediamine.
[i] mmsalH$_2$ = *meta*-methoxysalicylaldehyde.
[j] tpa = tris(2-methylpyridyl)amine.
[k] phaH$_2$ = propanohydroxamic acid.
[l] mmstH$_2$ = marimastat.
[m] 6-Ph$_2$tpa = *N*,*N*-bis((6-phenyl-2-pyridyl)methyl)-*N*-((2-pyridyl)methyl)amine.
[n] [12]aneN$_3$-mc2 = 2,4,4,9-tetramethyl-1,5,9-triazacyclododec-1-ene.
[o] bppa = *N*,*N*-bis[(6-phenyl-2-pyridyl)methyl]-*N*-[(6-pivaloylamido-2-pyridyl)methyl]amine.
[p] en = 1,2-diaminoethane.
[q] Tp^{Me,Ph} = hydrotris(5,3-methylphenylpyrazolyl)borate.
[r] pahaH = *N*-phenylacetohydroxamic acid.
[s] epahaH = *N*-(4-ethoxyphenyl)acetohydroxamic acid.
[t] phxhaH = *N*-phenylhexanohydroxamic acid.
[u] glyhaH$_2$ = glycinehydroxamic acid.
[v] Occurs as two crystallographically distinct anions.
[w] L″(1−) = *N*,*N*-dimethylhydroxylaminato.
[x] ombhaH$_2$ = 2-methoxybenzohydroxamic acid.
[y] mbhaH$_2$ = 4-methoxybenzohydroxamic acid.
[z] tfaH = trifluoroacetic acid; tfahaH$_2$ = trifluoroacetohydroxamic acid.

3.2. Mononuclear homoleptic complexes

One of the first structurally characterized metal–hydroxamic acid complexes was [Fe(bhaH)$_3$] [77]; the structure, as determined in 1969 (R = 0.12), and in subsequent work (R = 0.03 [78]; or R = 0.04 [79]) is a distorted octahedron with three *fac*-coordinated (previously annotated *cis*-) benzohydroxamato (bhaH) ligands (Fig. 2, **9**). In addition to *fac*- (**9**, **11**) and *mer*- (**10**, **12**) (previously annotated *trans*-) geometrical isomerism, octahedral tris-hydroxamato/imato complexes can exhibit optical isomerism (Δ or Λ). High-spin *rac*-[Fe(bhaH)$_3$] has been resolved into Δ-[Fe(bhaH)$_3$] and Λ-[Fe(bhaH)$_3$]: the resolution first involved the treatment of *rac*-[Fe(bhaH)$_3$] with base to form *rac*-[Fe(bha)$_3$]$^{3-}$ in solution which was then reacted with Δ- or Λ-[Co(en)$_3$]I$_3$ and the double salts isolated [80]. The Λ- or Δ-[Fe(bhaH)$_3$] isomers were subsequently obtained under acid extraction conditions and partitioned into an organic phase. Using a similar process, *rac*-[Ga(bhaH)$_3$] has been resolved into Λ- and Δ-[Ga(bhaH)$_3$], which is somewhat unexpected due to the lability of the Ga(III) d^{10} ion [81]. Mononuclear homoleptic complexes in which hydroxamic acids donate as dianions (hydroximato) include [B(bha)$_2$]$^-$ [82], *fac*-[Si(aha)$_2$]$^{2-}$, *fac*- and *mer*-[Si(bha)$_2$]$^{2-}$, *fac*- and *mer*-[Cr(bha)$_3$]$^{3-}$ [83], *mer*-[Co(bha)$_3$]$^{3-}$ [84] and *fac*-[Ge(bha)$_3$]$^{2-}$ [85].

The solid-state magnetic moments of Co(III)–hydroxamato complexes, such as [Co(bhaH)$_3$], are intermediate between

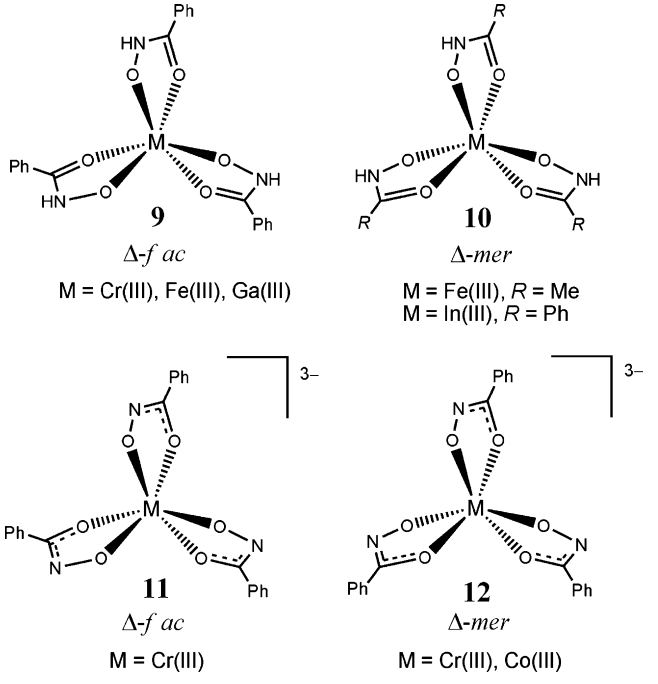

Fig. 2. Octahedral coordination (shown as the Δ-isomers) of tris-hydroxamato (*fac*-**9**, *mer*-**10**) or tris-hydroximato (*fac*-**11**, *mer*-**12**) complexes with M(III) ions as characterized by X-ray crystallography.

low and high-spin (2.7–3.6 μ_B), while $[Co(bha)_3]^{3-}$ and $[Co(bha)_2(bhaH)]^{2-}$ are diamagnetic [84]. The stronger ligand field posed by a hydroximato(2−) ligand (R_N = H), compared to the related hydroxamato(1−) ligand provides a rationale for this unusual case of proton-dependent spin-crossover. In $[Co(p\text{-}NO_2\text{-}bha)_3]^{3-}$, where the hydroximato ligand field strength is modulated by the electron-withdrawing nitro substituent, there is a switch from diamagnetism (solid state) to paramagnetism (aqueous solution), which indicates that the spin-crossover occurs after the second or third protonation event [84].

3.3. Mononuclear heteroleptic complexes

Many mononuclear heteroleptic complexes with bidentate *O*,*O*′-hydroxamato/imato coordination from monohydroxamic acids have been reported (Table 3). The majority of the heteroleptic bis-hydroxamato/imato complexes (oxo-V(V), Zn(II), *cis*-dioxo-Mo(VI), Rh(III), Sn(IV), *cis*-dioxo-W(VI)) have the M–OC bond in hydroxamato/imato chelate **1** *cis* to the M–OC bond in hydroxamato/imato chelate **2** [63,93–104]. The heteroleptic Si(IV)–hydroximato complexes $[(Me_2NH)CH_2Si(aha)_2]$ and $[(Me_2NH)CH_2Si(bha)_2]$ are zwitterionic with the trigonal-bipyramidal Si(IV) centre carrying a formal negative charge from two aha(2−) (or two bha(2−)) ligands and the (dimethylammonio)methyl(1−) ligand [105]. In $[(Me_2NH)CH_2Si(aha)_2]$, the (C)O–Si–O(C) bond angle is 176.8° [105]. In the seven-coordinate complex, *trans*-$[U(O)_2(MeOH)(pbha)_2]$, the single report of a U(VI)-hydroxamato complex characterized by X-ray crystallography, the (C)O–U–O(C) bond angle is 141.5° [106]. *cis*-Dioxo-Mo(VI) complexes have been isolated with $ahaH_2$ or $bhaH_2$, with selected complexes featuring a mixed hydroxamato/imato coordination mode. As would be expected for a mixed hydroxamato/imato complex, such as *cis*-$[Mo(O)_2(ahaH)(aha)]^-$, the M–ON and M–OC bond lengths in the hydroximato chelate are shorter than those in the hydroxamato chelate [100]. The mononuclear *cis*-MoO_2^{2+} complex, $[Mo(O)_2(glyhaH)_2]$ ($glyhaH_2$ = glycinehydroxamic acid) is noteworthy as an example of a complex in which the polyfunctional hydroxamic acid ligand coordinates the Mo(VI) ion in a 'regular' *O*,*O*′-bidentate fashion and not via the pendant amine group [99]. It is more usual for α- and β-amino hydroxamic acids to form polynuclear coordination complexes (metallacrowns) in which both the hydroxamic acid motif and the amine group are involved in metal coordination, with metal ions bridged by (*N*)*O* atoms (Section 3.5.2.). The only reported X-ray crystal structure for a W-hydroxamato complex is *cis*-$[W(O)_2(bhaH)_2]$ [104]. Complexes formed between the ligand, *N*,*N*-bis((6-phenyl-2-pyridyl)methyl)-*N*-((2-pyridyl)methyl)amine (6-Ph_2tpa), $ahaH_2$ and Co(II), Ni(II) or Zn(II) are mononuclear six-coordinate with ahaH(1−) coordinated as the monoanion [107]. The first Ru(III)–hydroxamato complex to be characterized by X-ray crystallography, $[Ru(edtaH_2)(ombhaH)]$ ($ombhaH_2$ = 2-methoxybenzohydroxamic acid), was prepared from the reaction in water between $K[Ru(edtaH)Cl]\cdot 1.5H_2O$ and $ombhaH_2$ [108]. At pH values >8.0, the hydroximato species $[Ru(edta)(ombha)]^{3-}$, is the dominant species in solution. One of the very few ever isolated Pu(IV) complexes has been synthesized with DFOE ($[Al(H_2O)_6][Pu(DFOE)(H_2O)_3]_2(CF_3SO_3)_5\cdot 14H_2O$) and has been characterized by X-ray crystallography [109].

Transition metals have been shown to mediate the reactivity of hydroxamic acids. The reaction between a 10-M excess of trifluoroacetic acid (tfAcOH) and $[Os(NO)_2(PPh_3)_2]$ yielded $[Os(tfaha)(tfAcO)(NO)(PPh_3)_2]$ ($tfahaH_2$ = trifluoroacetohydroxamic acid) which has been attributed to the *in situ* formation of tfaha(2−) from an intramolecular attack of a diprotonated NO ligand to the CO group of an Os-coordinated tfAcO(1−) [110]. The room temperature reaction between $K[Ru(edtaH)Cl]\cdot H_2O$ and $bhaH_2$ in aqueous solution resulted in the formation of $K_2[Ru(edta)(NO)Cl]$ with the Ru(II)–NO^+ motif characterized by the distinctive NO stretch in the infrared spectrum (ν_{NO} = 1880 cm^{-1}) [111]. The NO-donating ability of hydroxamic acids was illustrated in the same work in a biological system that measured the vascular relaxation of rat aorta via a NO-mediated activation of guanylate cyclase [111]. The reaction between $[Os(bpy)_2Br_2]$ and pbhaH yields an organometallic Os(III) complex, $[Os(bpy)_2(N\text{-phenylbenzamide}(1-))]^+$, with the Os(II) to Os(III) oxidation coupled to the reductive elimination of the OH group of the hydroxamic acid ligand [112]. In a related study, Rh(III) hydroxamato complexes were prepared by oxidation of the Rh(I) species, $[Rh(PPh_3)_3Cl]$, with pbhaH, which yielded $[Rh(pbha)_2Cl(PPh_3)]$ and amide byproducts [102]. Molybdenum(VI) has been used in a related ligand transformation (albeit in reverse) with the *N*-hydroxylation of phenacetin (*N*-(4-ethoxyphenyl)acetamide) to yield *N*-(4-ethoxyphenyl)-acetohydroxamic acid (epahaH) with the ultimate isolation of the bis-chelate *cis*-dioxo Mo(VI) complex, *cis*-$[Mo(O)_2(epaha)_2]$ [97]. In *cis*-$[Mo(O)_2(epaha)_2]$ and the related complex *cis*-$[Mo(O)_2(paha)_2]$ (pahaH = *N*-phenylacetohydroxamic acid), the M–OC groups are *trans* to each respective oxo group which results in significantly longer M–OC bond lengths, compared to the M–ON bond lengths [97]. A series of oxo/perox-Mo(VI) hydroxamato complexes, such as $[Mo(VI)(O)_2(cpha)]$ (cphaH = cinnamoyl-*N*-phenylhydroxamic acid), have been shown to catalyse the epoxidation of olefins with high catalytic conversions [113].

3.4. Bond lengths in mononuclear complexes

3.4.1. First coordination shell

In almost all of the hydroxamato/imato complexes characterized by X-ray crystallography, the M–OC bond is longer than the M–ON bond, although the magnitude of the difference varies among the metals and/or metalloid complexes. In bis- or tris-hydroxamato/imato complexes, this discussion relates to the M–OC and M–ON bond lengths as averaged over the two or three chelate rings, respectively. There are small differences in the M–OC and M–ON bond lengths in hydroxamato/imato complexes of Cr(III), low-spin hydroxamato/imato complexes of Co(III), the hydroxamato D_{3h} complex $[Ni([12]aneN_3\text{-}mc2)(ahaH)]^+$ ($[12]aneN_3$-mc2 = 2,4,4,9-tetramethyl-1,5,9-triazacyclododec-

1-ene) and in the hydroximato complexes of Si(IV), Ge(IV) and [Pt(shiH)(DMSO)$_2$]. The octahedral complex, [Ni(bppa)(ahaH$_2$)]$^{2+}$ (bppa = *N*,*N*-bis[(6-phenyl-2-pyridyl)methyl]-*N*-[(6-pivaloylamido-2-pyridyl)methyl]amine), is the only known case of a hydroxamic acid coordinating to a metal ion as a neutral ligand [118]; this binding motif is reflected in the longer M–O(H)N bond length (2.091 Å) compared to M–OC (2.037 Å). There is also a significant difference in the M–OC and M–ON bond lengths in the high-spin hydroxamato Co(II) complex, [Co(6-Ph$_2$tpa)(ahaH)]$^+$ [107].

The greatest differences in the M–OC and M–ON bond lengths is found in the oxo-V(V) and *cis*-dioxo-Mo(VI) and *cis*-dioxo-W(VI) complexes (Table 3); this marked inequivalence in bond lengths is likely due to the electronic effects imposed about the coordination sphere by the oxo group(s). In the mixed hydroxamato/imato complexes, *cis*-[Mo(O)$_2$(ahaH)(aha)]$^-$ [100] and [MoO(L(1−))(bha)(bhaH)] (L = *N*,*N*-dimethylhydroxylamine) [101], the M–OC bond of the hydroxamato ligand is *trans* to either the shorter of the two (*cis*-[Mo(O)$_2$(ahaH)(aha)]$^-$) or to the single ([MoO((CH$_3$)$_2$NO)(bha)(bhaH)]) oxo group(s). This M–OC bond length is significantly longer (average of ∼0.14 Å) that the M–OC bond length in the hydroximato chelate, which could be due to a combination of the *trans*-effect and the weaker donating ability of the hydroxamato(1−) versus the hydroximato(2−) ligand. In *cis*-[W(O)$_2$(bhaH)$_2$], *cis*-[Mo(O)$_2$(paha)$_2$] and *cis*-[Mo(O)$_2$(epaha)$_2$], the shortest M–OC bond is *trans* to the shorter of the two oxo-W(VI) or oxo-Mo(VI) bonds, which is unexpected in the context of the *trans*-effect. Therefore, in mixed hydroxamato/imato complexes, it appears that the charge on the ligand (hydroxamato/imato) directs the M–OC bond lengths to a greater extent than the *trans* effect. The M–OC bond length in [VO(shedH)(shiH)] (shedH$_2$ = *N*-(salicylideneaminato)-*N*′-(2-hydroxyethyl)ethylenediamine) is elongated due to its *trans*-disposition to the oxo group [95]. Fig. 3 shows the M–OC and M–ON bond length data from all the complexes in Tables 2 and 3, excluding the oxo-containing complexes (V(V), Mo(VI), W(VI), U(VI)) and the organometallic Sn(IV) complexes.

In mononuclear complexes with bidentate *O*,*O*′-coordination from monohydroxamic acids, there is a positive correlation between the increasing radius of the metal ion [122] and the increase in the length of both the M–OC (slope of line-of-best-fit (n = 17) = 1.01, R = 0.96) and M–ON (slope = 1.03, R = 0.96) bonds in hydroximato (Fig. 3a) and in hydroxamato (Fig. 3b) complexes (M–OC: slope of line-of-best-fit (n = 25) = 1.09, R = 0.95; M–ON: slope = 0.90, R = 0.92). Omitted from this analysis are oxo-containing hydroxamato/imato complexes and

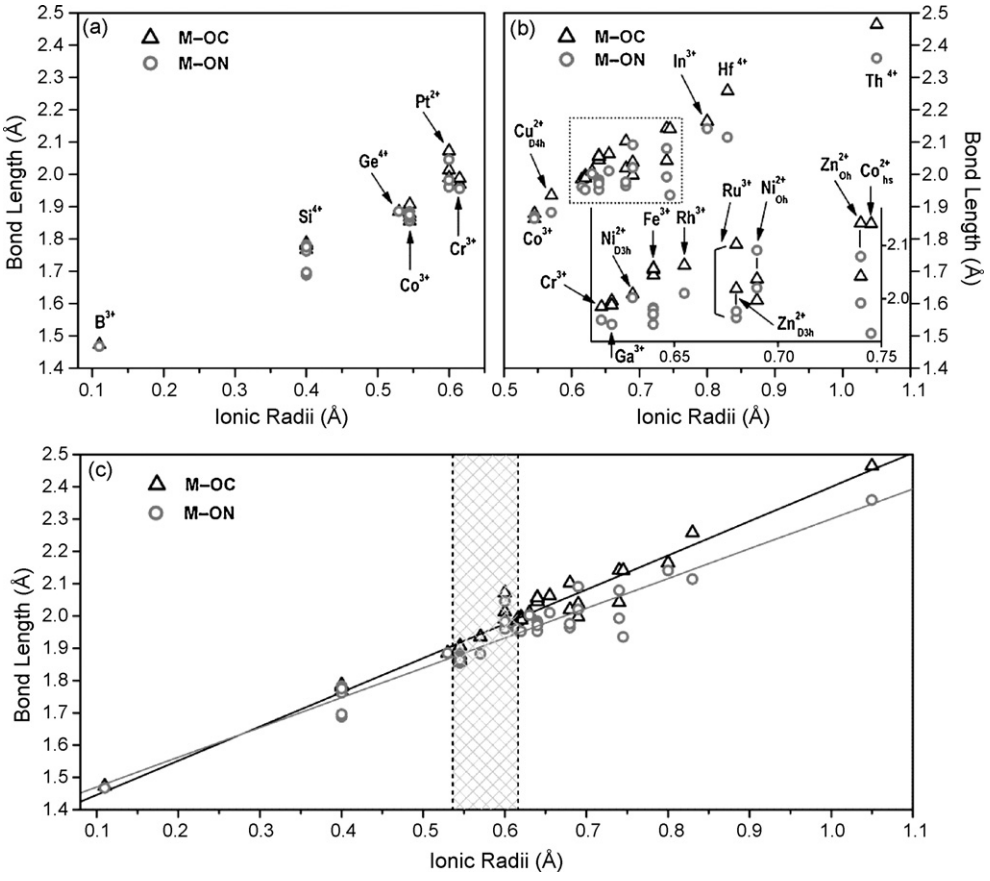

Fig. 3. Bond lengths (M–OC and M–ON) in non-oxo-containing mononuclear coordination complexes featuring bidentate (a) hydroximato or (b) hydroxamato ligands as a function of the metal ion radius. The boxed region in (b) has been expanded for clarity in the inset. Where practicable, for ions with multiple entries, dotted lines mark M–OC and M–ON bond lengths in a single complex. Panel (c) shows the hydroximato and hydroxamato data treated as a single pool with regression analyses and a hatched panel which represents the region of metal ion radii where hydroximato and hydroxamato complexes are found.

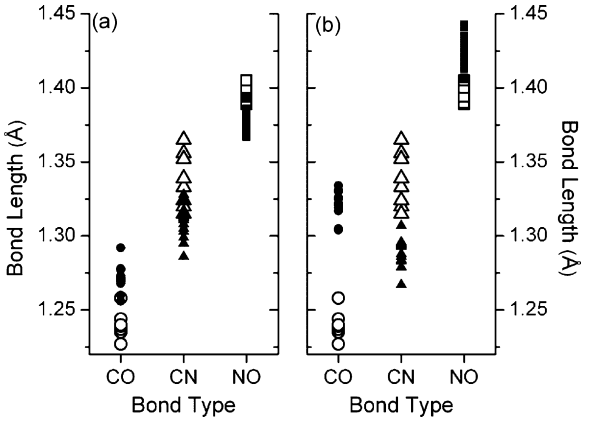

Fig. 4. Bond lengths (CO, CN, NO) in free hydroxamic acids (open symbols; $n = 8$) and corresponding bond lengths (closed symbols) in (a) hydroxamato ($n = 17$) or (b) hydroximato ($n = 14$) mononuclear coordination complexes.

the organometallic complex, $[(CH_3)_2Sn(mbhaH)_2]$, since in this complex, the average length of the M–OC bond (2.449 Å) suggests that the ligand is donating in a (*N*)*O*-monodentate fashion. The related complex, $[(CH_3)_2Sn(cbhaH)_2]$ ($pcbhH_2$ = *para*-chloro-benzohydroxamic acid), has similarly long M–OC bond lengths (2.597 Å and 2.330 Å; average = 2.463 Å); in the 'chelate' ring where M–OC = 2.597 Å, the ligand is monodentate [103]. If the data from both hydroximato and hydroxamato are pooled ($n = 42$), there is little difference in the regression analysis of the M–OC (slope of line-of-best-fit = 1.06, $R = 0.97$) or M–ON (slope = 0.92, $R = 0.96$) versus metal ion radius (Fig. 3c), compared to the case in which class of ligand is treated separately (Fig. 3a and b). Where the metal ion radius $\leq$0.53 Å or $\geq$0.62 Å all metal–hydroxamic acid complexes characterized by X-ray crystallography are hydroximato- or hydroxamato-based, respectively. Between the metal ion radii of 0.53 Å and 0.62 Å, is a region where both hydroximato and hydroxamato complexes have been characterized, as depicted by the hatched box in Fig. 3c. The correlation in metal ion radius and the formation of hydroximato or hydroxamato complexes is in broad agreement with hard–soft acid–base theory (HSAB), where the smaller, less readily polarisable metal ions with radii $\leq$0.53 Å will form stable complexes with the harder dianionic hydroximato ligand.

3.4.2. Second coordination shell

In both hydroxamato and hydroximato coordination complexes, the C–O bond length is longer compared to the corresponding bond length in the free ligand ($\Delta C{-}O_{complex-ligand} > 0$), with the difference significantly greater in hydroximato complexes, compared to hydroxamato complexes (Fig. 4). This indicates a greater C–O single bond character in hydroximato complexes, compared to hydroxamato complexes, which suggests that **3a** is the dominant resonance contributor in hydroximato complexes. The increase in the C–O bond length in both hydroxamato and hydroximato complexes is coupled to a decrease in the C–N bond length which indicates greater C–N double-bond character in both hydroxamato/imato complexes relative to the free ligand. The magnitude of the increase in the C–O bond length in hydroxamato/imato complexes, relative to the free ligand, correlates with the magnitude of the decrease in the corresponding C–N bond lengths: that is $|\Delta C{-}O_{complex-ligand}$ (hydroxamato/imato)$| \cong |\Delta C{-}N_{complex-ligand}$ (hydroxamato/imato)|. Also evident from Fig. 4 is $\Delta C{-}O_{complex-ligand}$ (hydroxamato) $< \Delta C{-}O_{complex-ligand}$ (hydroximato). The N–O bond length in hydroxamato complexes is smaller than the corresponding bond length in the hydroxamic acid free ligand. In hydroximato complexes, however, the N–O bond length increases relative to the free ligand. Taken together, the bond length data indicate that in coordination complexes, the dominant structures (Scheme 2) of hydroxamato complexes is **2a** and **2b** and of hydroximato complexes is **3a**. The data in Fig. 2 ($n = 17$, hydroxamato; $n = 14$, hydroximato) represents complexes with hydroxamic acids for which the structure of the free ligand is available (Table 1). Including bond length data from complexes in which the crystal structure of the free hydroxamic acid has not been solved ($n = 29$, hydroxamato; $n = 15$, hydroximato), finds a greater spread in the values of the C=O bond lengths in hydroxamato compared to hydroximato coordination complexes, which supports the presence of the two resonance contributors, **2a** and **2b**, although the spread could be due in part to the larger sample size of hydroxamato complexes.

3.5. Polynuclear complexes

3.5.1. Homometallic complexes

Two classes of homometallic dinuclear hydroxamate/imate complexes can be defined in which one class features an *O*-hydroxamate/imate atom μ-bridging between the metal ions and the other class features dihydroxamic acid ligands which coordinate in an *O*,*O*′-bidentate fashion to discrete metal ions. The dinuclear Ni(II) complex $[Ni_2(shiH)(shiH_2)(py)_4(OAc)]$ (Fig. 5, **13**), for example, belongs to the first class and features two $shiH_3$-derived ligands that bridge the two Ni(II) ions via two HN–O(1−) groups [123]. This complex is a striking model for the dinuclear Ni(II)-containing enzyme, urease (Section 4.1.), and is one of the few examples of a model complex of such accuracy preceding the solution of the X-ray crystal structure of ahaH(1−)-inhibited urease [16]. The Ni(II)···Ni(II) separation in **13** (3.016 Å) was thought likely to be less than would be expected in urease complexed with a single bridging hydroxamato ligand, which was borne out with the solution of the structure of ahaH(1−)-inhibited urease (Ni(II)···Ni(II) separation = 3.53 Å) [16] and in a related dinuclear Ni(II) compound (**14a**) with a bound urea ligand and single bridging hydroxamato (Ni(II)···Ni(II) separation = 3.434 Å) [124]. Two dinuclear Co(II) complexes have been reported with one (**14b**) or two (**15**) ahaH(1−) ligands bridging the Co(II) ions [125]. The dinuclear complex $[Zn_2(\mu\text{-}OAc)_2(OAc)(\mu\text{-}bhaH)(tmen)]$ (tmen = *N*,*N*,*N*′*N*′-tetramethylethylenediamine) [126] has a coordination geometry (**16**) that is a good model of the *p*-iodo-D-phenylalanine hydroxamic acid-inhibited dinuclear Zn(II)-containing aminopeptidase from *Aeromonas proteolytica* [127]. The Mn(II) complex with

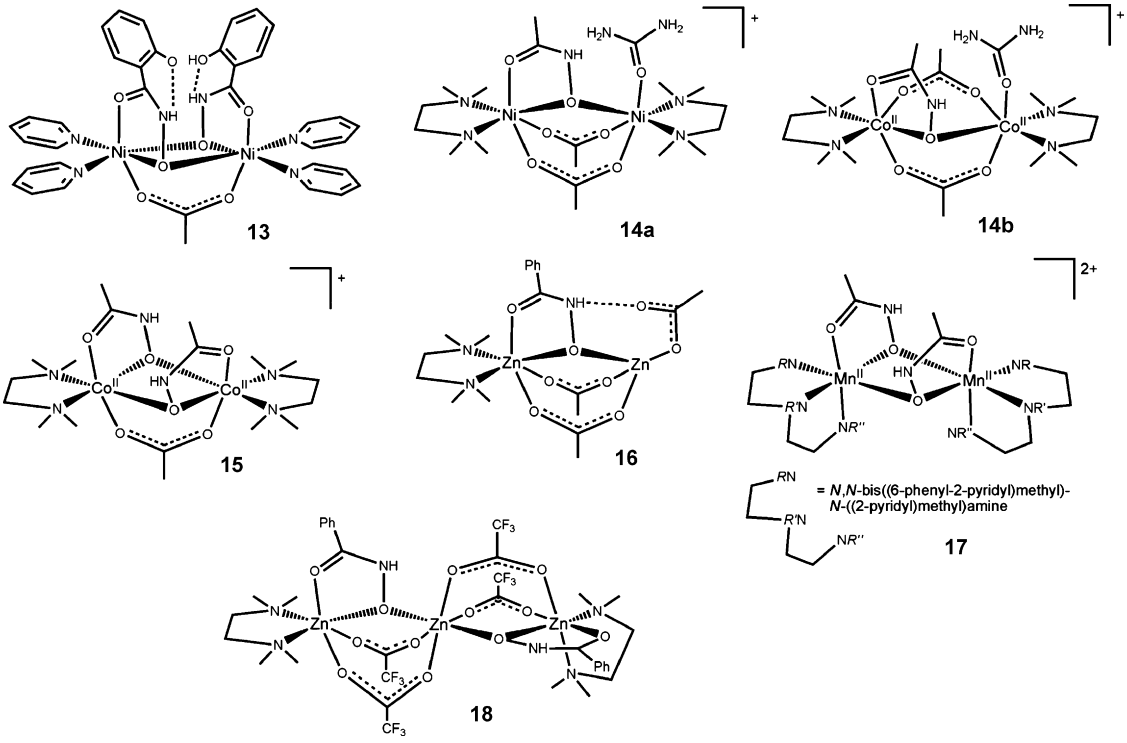

Fig. 5. Di- and tri-nuclear homometallic complexes with μ-*O*-bridging hydroxamic acid coordination: **13** [123], **14a** [124], **14b** [125], **15** [125], **16** [126], **17** [107], **18** [129].

6-Ph_2tpa and acetohydroxamic acid is dinuclear (**17**) with two acetohydroxamato (ahaH(1−)) ligands bridging the Mn(II) ions (Mn(II)···Mn(II) separation = 3.409 Å) and, discounting the metallacrowns (Section 3.5.2.), is the first structurally characterized Mn(II)-hydroxamato complex [107]. The synthetic strategy adopted for **15** (and other related complexes) involved the facile reaction between the preassembled dinuclear complex $[Co_2(\mu\text{-}H_2O)(\mu\text{-}OAc)_2(OAc)_2(tmen)_2]$ and $ahaH_2$ [125]. When the starting homometallic (M(II)) dimer (M = Co, Ni) featured trifluoroacetate ligands rather than acetate ligands, the reaction with $ahaH_2$ or $bhaH_2$ yielded novel trinuclear complexes [128]. The acidity of the bridging ligand appears to play a significant role in directing the nuclearity of the final complex. The trinuclear Zn(II) complex $[Zn_3(tfAcO)_4(tmen)_2(bhaH)_2]$ (**18**) features two tmen ligands which cap the outer Zn(II) ions and two pairs of trifluoroacetate ligands that bridge between the central Zn ion and the flanking Zn ions. Two bhaH(1−) ligands form μ-*O*-bridging ligands between pairs of Zn(II) ions akin to related dinuclear complexes [129].

Two dinuclear homometallic complexes with V(V) or Cu(II) and the dihydroxamic acid ligand, *N*,*N*′-dihydroxy-*N*,*N*′-diisopropylheptanediamide, have been characterized by X-ray crystallography [93,130]. In both complexes, each dihydroxamic acid unit flanking the pentane core, coordinates to a discrete metal ion in a *O*,*O*′-hydroxamato fashion. In the case of the Cu(II) complex (**19a**), a second ligand coordinates in a *cis*-fashion to yield a complex with square planar geometry at each metal site with a distance between the Cu(II) ions of 6.256 Å. Magnetic susceptibility measurements ($\mu_B = 1.80$ per Cu(II)) show no significant magnetic interaction between the Cu(II) ions [130]. In the case of the V(V) complex, the second *N*,*N*′-dihydroxy-*N*,*N*′-diisopropylheptanediamide ligand coordinates in a fashion similar to that for the Cu(II) complexes to give a centrosymmetric dimer (**19b**) with additional *cis*-coordinated monodenate oxo(2−) and isopropanoato(1−) ligands at each metal ion (separated by 11.09 Å) to give an octahedral coordination environment [93] (Fig. 6).

The reaction between 2-(dimethylamino)phenylhydroxamic acid and Ni(II) produced a heptanuclear Ni(II) complex with

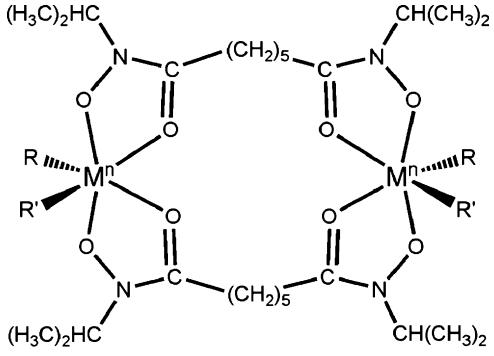

Fig. 6. Dinuclear homometallic complexes with *O*,*O*′,*O*″,*O*‴-dihydroxamate coordination: **19a** [130], **19b** [93].

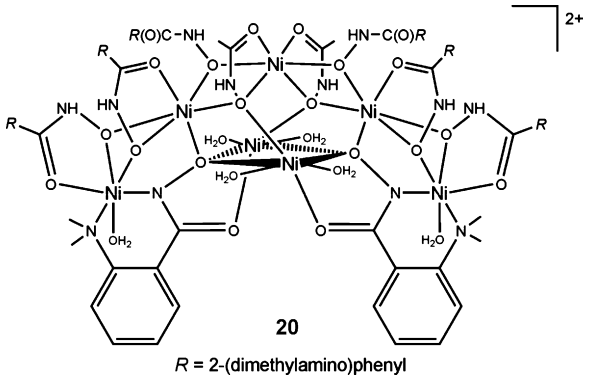

Fig. 7. Heptanuclear Ni(II)-2-(dimethylamino)phenylhydroxamic acid complex [131].

a croissant-like architecture (Fig. 7, **20**) with extensive bridging from the amidohydroxyl group of 10-mole equivalents of hydroxamic acid (eight hydroxamato and two hydroximato ligands) between two, three or four clustered Ni(II) ions, each of which are in a distorted octahedral environment [131]. Overall, the complex is weakly antiferromagnetic between 4 K and 300 K with a room temperature $\mu_{eff} = 7.93\mu_B$ [131]. A highly bridged Ni(II) cluster has also been prepared from a mixed-ligand system in which one of the ligands is $shiH_3$ [132].

The reaction between Cu(II) and 3-aminobenzohydroxamic acid yielded $[Cu_3(3\text{-}NH_2\text{-}bhaH)_4(H_2O)SO_4]_n{\cdot}8H_2O$ which forms a helical polymer with an extensive hydrogen bond network linking the polymer chains [133]. *Ortho*- or *para*-substitution of the amino group of $bhaH_2$ yielded a strongly antiferromagnetic ($\mu_{eff} = 4.0\mu_B$) dimeric metallacrown-type complex, $[Cu_5(2\text{-}NH_2\text{-}bha)_4\text{-}(\mu\text{-}SO_4)(H_2O)_2]_2{\cdot}10H_2O$, or a mononuclear Cu(II) complex, $[Cu(4\text{-}NH_2\text{-}bhaH)_2]{\cdot}H_2O$, respectively [133].

3.5.2. Metallacrowns

Polyfunctional hydroxamic acids are known to form polynuclear metal–ligand clusters, known as metallacrowns, which are structurally analogous to crown ethers. The mixed-valence Mn(II)–Mn(III) metallacrown formed with $shiH_3$ features a 12-metallacrown-4 [12-MC-4] core structure and a central Mn(II) ion sitting 1.20 Å above the metallacrown plane (Fig. 8, **21**). Each $shiH_3$ ligand is triply deprotonated with the hydroximato ligand chelating one Mn(III) ion and the amidohydroxylato N atom and the phenolato O atom of the same shi(3−) ligand coordinated to an adjacent Mn(III) ion [134]. Metallacrown complexes featuring Ni(II) and $shiH_3$ or 2-picolinehydroxamic acid have been characterized in solution and by X-ray crystallography [132,135–137].

The first Cu(II) [12-MC-4] complex characterized by X-ray crystallography (**22**) shows β-alanine hydroxamic acid acting as a tridentate chelate, via the polydentate hydroximato group and the pendant amine [138]. In a fashion akin to the trispyrazolylborates [139], the ligand is acting in a scorpion-like fashion with the hydroxamato 'pincers' and the pendant amine 'sting'. Indeed, the C_s symmetry of a scorpion is better represented by the pseudo C_s symmetry of the β-alanine hydroxamic acid ligand compared to the original 'scorpionate' ligands of C_3 symmetry. β-Aminohydroxamic acids form [12-MC-4] systems with fused 5- and 6-membered rings (**21**, **22**), while α-aminohydroxamic acids form 15-metallacrown-5 systems ([15-MC-5], **23**). The larger cavity size of the [15-MC-5] complexes are tuned toward the encapsulation of Ln(III) ions, such as Gd(III), Eu(III), or Sm(III) or uranyl ions [140–142]. Based upon ^{1}H NMR, CD and ESI-MS spectroscopic results, the titration of a solution of a Ln(III) salt into a solution of **22** converts the parent homometallacrown to the Ln(III)[15-MC-5] heterometallacrown (**23**) complex [143]. Several excellent reviews focus exclusively upon metallacrowns and the molecular recognition properties of these compounds [144–146]. The use of aminohydroxamic acids gives rise to the potential for the exploitation of chiral recognition properties and has lead to several remarkable helical structures, as for example between Cu(II) and L-norvaline [147].

3.6. Atypical modes of coordination

The reaction between $bhaH_2$ and $[Fe(oep)]_2(\mu\text{-}O)$ (oep = octaethylporphyrin) yielded $[Fe(oep)(bhaH)]{\cdot}bhaH_2$ [148] in which the benzohydroxamato coordinates to the Fe(III) as a unidentate ligand via the amidohydroxylato group (Fig. 9, **24**). This is the only example in the coordination chemistry literature that describes the monodentate coordination of a hydroxamic acid to a metal ion.

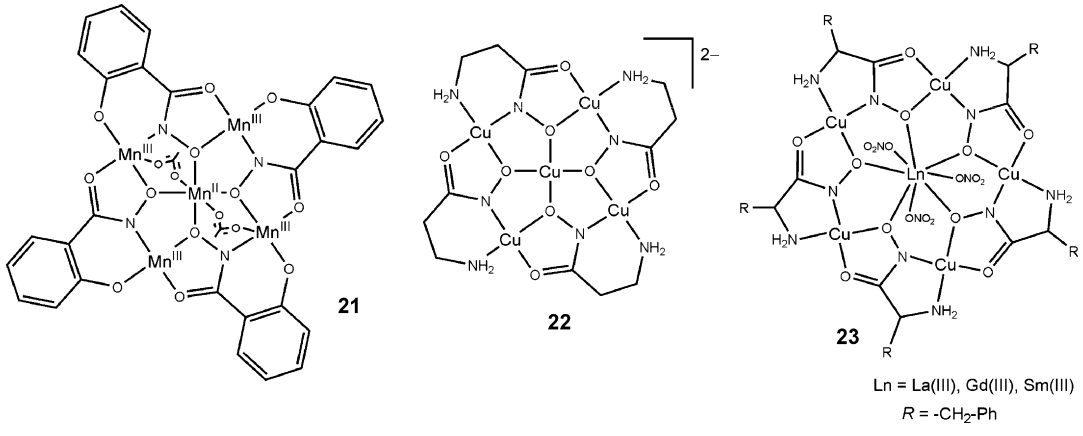

Fig. 8. Homometallic (**21** [134], **22** [138]) and heterometallic (**23** [143]) metallacrowns.

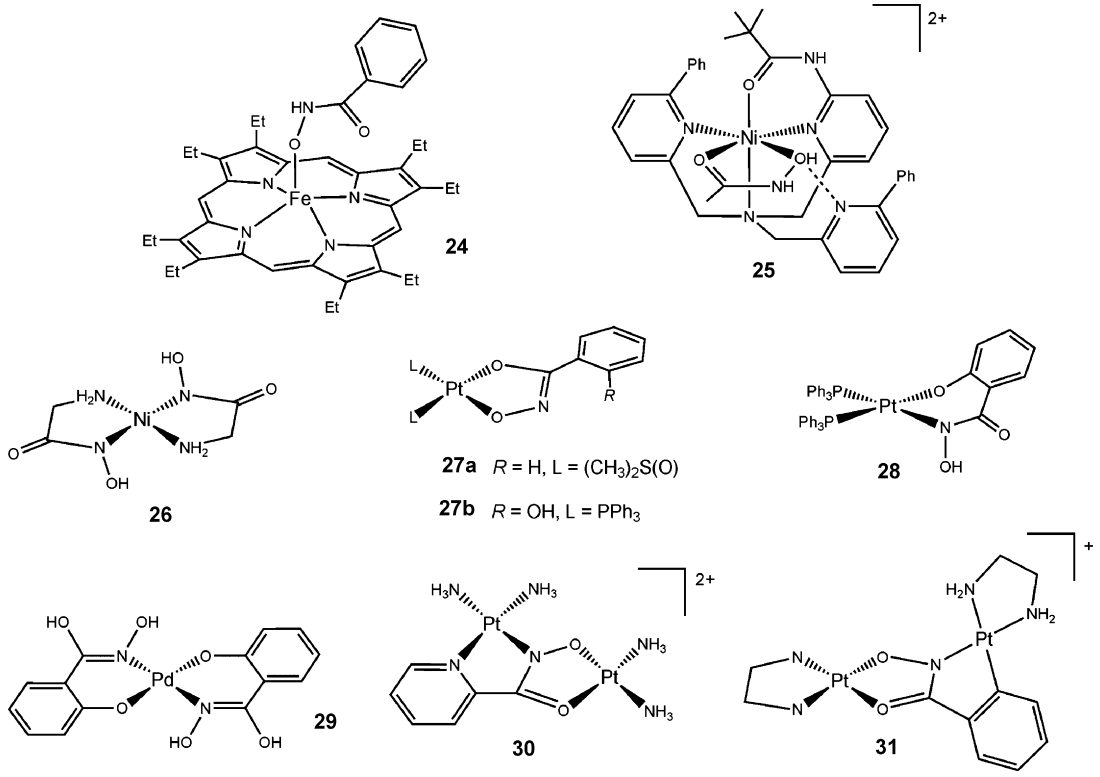

Fig. 9. Atypical coordination modes in hydroxamic acid complexes: **24** [148], **25** [118], **26** [149], **27a** [121], **27b** [120], **28** [151], **29** [120], **30** [152], **31** [154].

Acetohydroxamic acid binds as a neutral donor to a mononuclear Ni(II) centre in $[Ni(bppa)(ahaH_2)]^{2+}$ (**25**) [118]. This is the only case known in classic coordination chemistry in which a hydroxamic acid is not deprotonated upon metal binding; the Ni–O(H)N and Ni–O(C) bond lengths (2.091 Å and 2.037 Å, respectively) are consistent with the notion of the ligand neutrality; there is a intramolecular hydrogen bond from the O(H)N group to the N atom of the non-coordinated pyridyl group (O–H···N of 2.518 Å). The Ni–O(H)N bond length in IV (2.091 Å) is longer that the Ni–ON bond length (2.020 Å) in a related structure in which ahaH(1−) coordinates as a monoanion [107]. The complex formed between Ni(II) and glycinehydroxamic acid is noteworthy [149] in the metal coordination via the N atom of the amidohydroxyl group (**26**), rather than as a *O,O′*-bidentate chelate. In the crystal structure of $[PPh_4]_2[Ni(pydhaH_2)_2]$ ($pydhaH_4$ = pyridine-2,6-dihydroxamic acid), coordination to Ni(II) occurs via the pyridyl N atom and two deprotonated N atoms from each $pydhaH_2(2-)$ chelate [150].

Salicylhydroxamic acid exhibits coordination isomerism in Pt(II) or Pd(II) complexes with the coordination mode directed by the synthetic route and by the ancillary ligands of the starting Pt(II) complex [151]. The reaction between *cis*-$[PtCl_2(L)_2]$ and $bhaH_2$ (L = DMSO) or $shiH_3$ (L = PPh_3) in the presence of base gave $[Pt(bha)(DMSO)_2]$ (**27a**) or $[Pt(shiH)(PPh_3)_2]$ (**27b**), respectively, in which the hydroxamic acid coordinates to the Pt(II) centre as an *O,O′*-dianion [120,121]. In **27b**, there is a intramolecular hydrogen bond between the protonated phenol group and the second-coordination sphere N atom which confers planarity upon the complex [120]. The addition of an excess of PPh_3 to [Pt{OPhC(O)NOH}(cod)] (cod = cycloocta-1,5-diene) in which shiH(2−) coordinates to Pt(II) through the phenolate O atom and the N atom of the N–OH group yields **28** [151] as a coordination isomer of **27b**. The reaction between $K_2[PdCl_4]$ and $shiH_3$ gives $[Pd(shiH_2)_2]$ (**29**) in which $shiH_2(1-)$ coordinates in the *N,O*-chelate yielding six-membered chelate rings with two intramolecular hydrogen bonds occurring from the deprotonated phenolate O atom in one ring to the proton of the amidohydroxyl group of the opposite ring [120]. The average length of the C–N bond (1.294 Å) reflects the considerable C=N double bond character [120] and approximates the hydroxamic acid tautomer **1c** (Scheme 2). The reaction between *cis*-$Pt(II)(NH_3)_2(NO_3)_2$ and picolinohydroxamic acid (2-pyridinehydroxamic acid) ($pihaH_2$) gave upon addition of $NaClO_4$ the dinuclear Pt(II) complex, $[\{cis\text{-}Pt(NH_3)_2\}_2(\mu\text{-piha})](ClO_4)_2\cdot H_2O$ [152]. In this complex (**30**), one Pt(II) site features *O,O′*-bidentate chelation from the picolinohydroximate ligand and the second Pt(II) site is *N,N′*-coordinated via the imato and pyridine groups [152]. Heterobimetallic Pt(II)/M(II) (M = Cu, Ni or Zn) complexes have been formed using nicotinohydroxamic acid (3-pyridinehydroxamic acid) or isonicotinohydroxamic acid (4-pyridinehydroxamic acid), in which the hydroxamate ligand bridges between Pt(II) and M(II) to form a novel wave like coordination polymer [153]. A two-membered family of novel organometallic dinuclear Pt(II) hydroxamic acid complexes have been characterized by X-ray crystallography [154] in which a Pt(II)–C bond is formed from the aromatic ring of a triply deprotonated $bhaH_{-1}$ ligand which bridges between the Pt(II) centres (**31**). Indeed, while non-*O,O′*-bidentate coordination of hydroxamic acids may be

thought of as 'atypical', *N*,*N*′- and *O*,*N*-binding modes for the softer metal ions, Pt(II) and Pd(II), particularly in complexes with polyfunctional hydroxamic acids (shiH_3 or pyhaH_2) are rather more common.

3.7. Solution chemistry

There have been extensive studies on metal–hydroxamato/imato species formed in solution, with most studies focused upon the metal complexation of naturally occurring hydroxamate-based siderophores, such as DFOB [155]. Fewer studies have focused upon the complexes formed in solution between metals and simple monohydroxamic acids. Complexes between Fe(III) and ahaH_2 or bhaH_2 are formed in solution at acidic pH values; where there is large excess of ligand, the octahedral 1:3 Fe(III):hydroxamato complexes are formed between pH values between 4 and 8 [156]. The log β_{130} values of [Fe(aha$H$)$_3$], [Fe(bha$H$)$_3$] and [Fe(pbha)$_3$] range between 28.44 and 28.80 [2,156]. The thermodynamics of Fe(III)–hydroxamato complex formation has been shown to depend upon the electronic properties of the R_C and R_N groups [60,61]. An electron donating group at R_N increases the strength of the C(O)–M bond via the delocalization of the C=N electrons onto the carbonyl group, thereby increasing the stability of the complex [60,61]. The high stability constants of Fe(III) complexes with ahaH_2 or bhaH_2 is borne out by the ability of each of these ligands to complex with Fe(III) in iron-loaded ferritin [157]. In this work, it was shown that ahaH_2 or bhaH_2 was able to diffuse into the channels of ferritin, coordinate Fe(III) and to exit the channels (which are approximately 4 Å in diameter) as either a mono- or bis-hydroxamato-Fe(III) complex [157]. This direct leaching of Fe(III) by a small ligand is distinct from the mechanism for Fe(III) mobilization from ferritin which proceeds via Fe(III) to Fe(II) reduction. The Fe(III) release was maximized with ahaH_2 (relative to bhaH_2) and at acid pH values (pH 5.2 > pH 7.4) and in the presence of urea [157]. Coordination modes in solution have been studied for Cu(II)– or oxoV(IV)–hydroxamato complexes [156,158], in mixed-ligand Cu(II), Ni(II) and Zn(II) complexes [159] and for complexes formed in solution between Ga(III) or In(III) and bhaH_2 or pbhaH [160] and Ni(II) with pbhaH [58]. The solution speciation of VO^{2+} or VO^{3+} or VO_2^+ with hydroxamic acids is of interest in the context of work which has shown the inhibition of the β-lactamase of *Enterobacter cloacae* P99 by 1:1 complexes of V(V) and hydroxamic acids [161] and in terms of the insulin mimetic properties of oxoV(V/IV)–hydroxamic acid species [114]. Complexes formed between oxo-Cr(V) (d^1) and ahaH_2, bhaH_2 and the linear dihydroxamic acid, suberodihydroxamic acid, have been characterized in solution using EPR spectroscopy [162]. Speciation between Mo(VI) and ahaH_2, bhaH_2 or *N*-methylacetohydroxamic acid has been studied by ^{1}H and ^{17}O NMR spectroscopy and stability constants calculated for [MoO_2L_2] and [MoO_3L]$^-$ (L = ahaH_2) of log β = 32.46 and 17.16, respectively [163]. Studies using potentiometric titrations have determined the solution equilibria of Fe(III), Ga(III), In(III), Al(III) or Ni(II) with dihydroxamic acids [164,165]. To meet octahedral coordinative saturation in the case of Fe(III), the stoichiometry of Fe:dihydroxamic acid complexes is 2:3 [164,165] which is the stoichiometry also borne out in solution and solid state studies of the Fe(III) complex formed with the naturally occurring dihydroxamic acid, alcaligin or rhodotorulic acid [166–168]. The citrate-based dihydroxamic acid, aerobactin, which is sourced from marine and terrestrial organisms, has been shown to be photoreactive, with the decarboxylation of the central carboxylate group yielding a keto–enol derivative with Fe(III) binding properties that approximately mimic the properties of the parent siderophore [169]. The Fe(III)–DFOB complex, in which the pendant amine tail is positively charged at pH values <10.8, has a log β_{110} = 30.6 [165,170]; for complexes formed between DFOB and Ga(III) or Al(III), the log β_{110} = 28.2 or 24.1, respectively [165]. The complexation between Pu(IV) and DFOB in solution has recently been examined in the context of the ability of siderophores leached into the environment for bioremediating contaminated sites. This study showed that at [Pu(IV)]:[DFOB] = 1:1, the dominant species at neutral pH is [Pu(DFOB)(OH)]$^+$ [171]. In solutions containing equimolar [Pu(IV)], [DFOB] and [Fe(III)] at pH values >4, the dominant species is [Fe(DFOB)]$^+$ [171] even though the stability of [Pu(DFOB)]$^{2+}$ (log β_{110} = 33.98) is greater than that of [Fe(DFOB)]$^+$. The solution speciation of metal–hydroxamato/imato complexes is of significance in terms of reaching a more complete understanding of how these bioligands interact with the active site of metalloproteins and by translation, the use of hydroxamic acids as metalloproteins inhibitors in pharmacological applications.

4. Hydroxamic acid complexes in chemical biology

The rich coordination chemistry of hydroxamic acids, in terms of the number of complexes characterized by X-ray crystallography and the solution chemistry (Section 3) suggests that these ligands may also coordinate active site metal ions in metalloproteins. The coordination of monohydroxamic acids to several Zn(II)- or Ni(II)-containing metalloenzymes has been studied by X-ray crystallography. The enzymes studied include urease (binuclear Ni(II)-containing) and Zn(II)-containing enzymes, including matrix metalloproteinases (MMPs), aminopeptidases, anthrax lethal factor, botulinium neurotoxin and carbonic anhydrase. X-ray crystallography has also proven a useful tool for examining the binding between Fe(III)-loaded polyhydroxamic acids and cognate binding proteins that are integral to prokaryotic Fe(III)-uptake mechanisms.

4.1. Ni(II)-dependent systems

Hydroxamic acids have been long known to inhibit urease, a dinuclear Ni(II)-containing enzyme, which catalyses the hydrolysis of urea to ammonia and carbamate [172]. In the X-ray crystal structure of aha$H$(1−)-bound urease from *Bacillus pasteurii* (Fig. 10), the amidohydroxylato group of the acetohydroxamato ligand bridges between the two Ni(II) atoms in the dinuclear active site [16] which replaces a bridging hydroxyl group in native urease. Donation from four histidine residues (two per

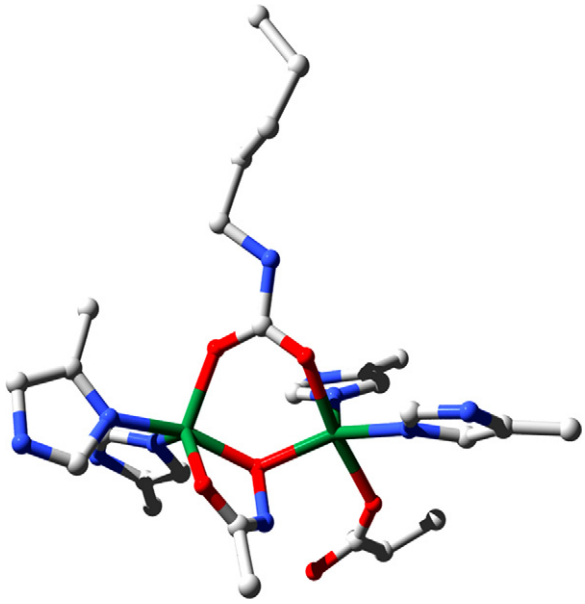

Fig. 10. Active site (hydrogen atoms omitted for clarity) of acetohydroxamato-bound urease (Ni(II)) from *Bacillus pasteurii* [16]. Figure generated using Swiss-PdbViewer v3.7 [175] and POV-Ray v3.6 [176].

Ni(II)), a bridging carbamylated lysine residue and a mondentate carboxylate (Ni2) or the CO group from ahaH(1−) (Ni1) gives a five-coordinate geometry at each Ni(II). The trigonal-distortion parameters, τ(Ni1) = 0.363 and τ(Ni2) = 0.365, indicate greater trigonal bipyramidal character [173] relative to the geometry of the active-site Ni(II) ions in *B. pasteurii* urease bound to diamidophosphate or β-mercaptoethanol. A hydrogen bond (2.6 Å) exists between the NH group of ahaH(1−) and the non-coordinated O atom of the Asp group. A similar coordination environment is observed at the dinuclear Ni(II) centre in the X-ray crystal structure of ahaH(1−) bound to a recombinant mutant of urease from *Klebsiella aerogenes* [174].

4.2. Zn(II)-dependent systems

Many X-ray crystal structures report the coordination of hydroxamic acids to the catalytic Zn(II) site in matrix metalloproteinases (MMPs). Matrix metalloproteinases are a family of Zn(II)-containing endopeptidases which play roles in the regulation of the structures of extracellular matrices. The overexpression and/or misregulation of MMPs (collagenase, gelatinase, stromelysin, matrilysin, metalloelastase) has pathological implications in diseases including rheumatoid and osteoarthritis, metastasis and emphysema. Hydroxamic acids inhibit MMPs by binding to the catalytic Zn(II) site which has fueled research into the design of hydroxamic acid-based drugs with superior zinc-binding groups (ZBG) for the treatment of MMP-related diseases [23–25].

There is a characteristic binding motif between hydroxamic acids and the catalytic Zn(II) site of MMPs. First, the ahaH$_2$ or *C*-substituted analogue (**1**: R_C = alkyl/aryl, R_N = H) coordinates to the catalytic Zn(II) ion in a *O*,*O*′-bidentate fashion as a neutral donor with three histidine-derived nitrogen atoms from the zinc-binding sequence motif (HExxHxxGxxH) saturating the overall Zn(II) trigonal-bipyramidal active-site geometry. Second, there is a hydrogen bond formed between the NO–H hydrogen atom of the coordinated hydroxamic acid and the O atom(s) of a proximal glutamic acid residue of a distance ranging between 2.4 Å and 3.1 Å. Third, in many (but not all) of the structures, there is an additional hydrogen bond interaction between the hydroxamic acid NH group and the amide O atom of a distal alanine residue (Fig. 11, **32a**) [18–22]. Structurally complex hydroxamic acid-based inhibitors, such as batimastat, show many additional hydrogen bonds and hydrophobic interactions upon binding to Zn(II) in MMP-12 [177]. The structures of ternary ahaH$_2$-MMP-12-inhibitor (non-hydroxamato-based) complexes have also been described in which the binary ahaH$_2$-MMP-12 complex directs the solubility and IC$_{50}$ properties of the ternary complex [178].

Hydroxamic acids coordinate to the Zn(II) active site in anthrax lethal factor [179,180] or botulinum neurotoxin serotype A [181] in a fashion similar to the ligand-bound MMP systems with changes to the Zn(II)-coordinated residues (His to Glu) and in select cases [179] to the residue interacting via the amide CO group with the NH proton (Ala to Gly) (**32b**). The aryl hydroxamic acid, *N*-hydroxy-4-{methyl[(5-pyridin-2-yl-2-thienyl)sulfonyl]amino}benzamide, binds to the Zn(II) site (His, Asp, Asp) in human histone deacetylase (HDAC8) via the *O*,*O*′-bidentate group (**33**) with hydrogen bond interactions between each of the NHOH protons and two histidine residues

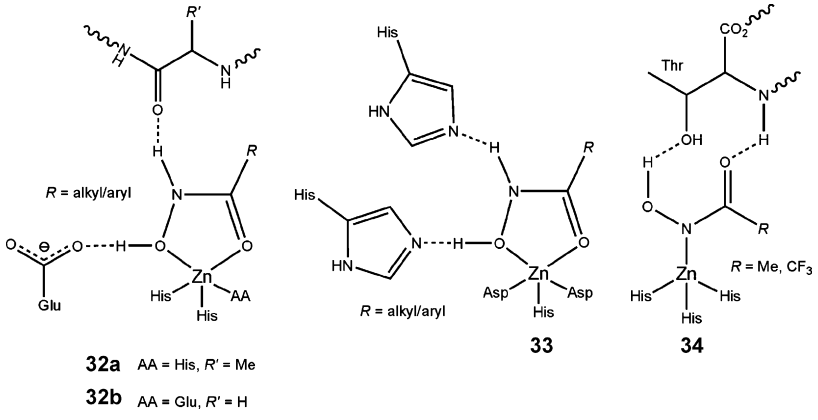

Fig. 11. Coordination motifs of hydroxamic acids bound to Zn(II)-containing metalloproteins as determined from X-ray crystallography.

[182] in a fashion similar to other HDAC8 structures with bound hydroxamic acids [183,184].

Crystals of carbonic anhydrase soaked in ahaH$_2$-containing solutions revealed the acetohydroxamato ligand coordinated to Zn(II) via the deprotonated N atom (Zn(II)–N bond length = 1.964 Å), which is a unique hydroxamato-metal binding mode in biology [17], although this coordination mode has been illustrated in a hydroxamic acid complexes with Ni(II) (**25**) [118]. Coordination between tfahaH$_2$ and the Zn(II) ion in carbonic anhydrase reveals a polar interaction between the Zn(II) ion and the F atom (Zn···F = 2.8 Å) which may stabilize the metal–ligand complex (Fig. 11, **34**).

A hydroxamato-bridged structure reminiscent of ahaH(1−)-bridged urease, has also been observed between *p*-iodo-D-phenylalanine hydroxamato and the dinuclear Zn(II)-active site of aminopeptidase from *Aeromonas proteolytica* [127]. In this structure, the amidohydroxylato group bridges between the two Zn(II) ions with a further Asp-derived carboxylate bridge and His/Asp donation or His/Glu donation at each respective Zn(II) site [127]. The dinuclear Zn(II) complex **16** models this hydroxamato-bound metalloenzyme active site [126].

4.3. Fe(III)-dependent systems

The Fe(III)-dependent hydroxamic acid systems in chemical biology relate to the small molecule siderophores that coordinate Fe(III) with high affinity and selectivity and to the cognate Fe(III)–siderophore receptor proteins at the bacterial cell surface that must recognize the Fe(III)–siderophore complex for downstream processing. There are an increasing number of X-ray crystal structures of Fe(III)–siderophores and of the Fe(III)–siderophore–protein ternary complexes. There are several structures of Fe(III) complexes with naturally occurring linear trihydroxamic acids or cyclic di- or trihydroxamic acids. The saturated octahedral Fe(III) coordination environment is met for a trihydroxamate with an Fe(III):ligand ratio of 1:1. In the case of dihydroxamic acids, the more commonly observed stoichiometry at neutral pH values is Fe(III):ligand of 2:3. The X-ray crystal structure of the Fe(III) complex of the 20-membered cyclic dihydroxamic acid, alcaligin, for example, reveals a Fe(III):ligand ratio of 2:3 with a U-shaped conformation [168]. The average Fe–O(C) and Fe–O(N) bond lengths in Fe$_2$alcalgin$_3$ are 2.045 Å and 1.978 Å, respectively [168], which are close to the related bond lengths observed in small molecule Fe(III)–hydroxamate complexes (Table 3). The only detectable difference in the first (M–ON, M–OC) and second (C–O, C–N, N–O) coordination sphere bond lengths of Fe(III) complexes formed with monohydroxamic acids (Table 2) or naturally occurring polyhydroxamic acids (Table 4) is in the C–O–M region of the chelate ring. An increase of approximately 0.01 Å in the C=O bond length in Fe(III)–polyhydroxamato complexes, relative to Fe(III)–tris-monohydroxamato complexes, is coupled with a decrease of similar magnitude in the M–OC bond length. The O–Fe–O bond angles are also similar between these two classes of Fe(III)–hydroxamato complexes [185]. The M–ON (2.305 Å) and M–OC (2.362 Å) bond lengths in the nine-coordinate Pu(IV)–DFOE complex [109] are significantly longer than in the Fe(III) analogue; the diameter of the Pu(IV)–DFOE and Fe(III)–DFOE complexes, however, do not vary significantly, which attests to the conformational flexibility of the family of cyclic trihydroxamic acids.

The crystal structure of ferrioxamine B (the Fe(III)-loaded form of desferrioxamine B) bound to the hydroxamato-type iron-siderophore periplasmic transport protein from *E. coli* (FhuD) has been solved to 1.97 Å resolution [191]. A comparison of the X-ray crystal structures of free ferrioxamine B (FOB) [185] and of FOB complexed with the periplasmic transport protein, FhuD from *E. coli* reveals several interesting differences. First, the configuration of FOB according to the single crystal X-ray analysis (Fig. 12) is a racemic mixture of the Δ-*N-cis*, *cis* (**35a**) and Λ-*N-cis*, *cis* isomers (**35b**) [185]. Indeed, all of the Fe(III)–ferrioxamine structures (Table 4) crystallize as racemic mixtures of Λ- and Δ-*cis* isomers [185]. It is noteworthy that the configuration of FOB in the binary FOB–FhuD complex (2.0 Å resolution) is Λ-*C-trans*, *cis* (**35c**). This shows that the

Table 4
Selected average bond lengths (Å) in complexes with bidentate *O*,*O*′-hydroxamato/imato coordination from naturally occurring polyhydroxamic acids

Complex[a]	Average bond length (Å)					Reference
	C–O[c]	C–N	N–O	M–ON	M–OC	
[Fe$_2$(alcaligin)$_3$]	1.280	1.313	1.383	1.978	2.046	[168]
[Fe(DFOB)]$^+$	1.284	1.315	1.376	1.978	2.036	[185]
[Fe(DFC)]	1.278	1.305	1.389	1.983	2.034	[186]
[Fe(DFCA)]	1.265	1.326	1.372	1.980	2.033	[186]
[Fe(DFOD$_1$)]	1.275	1.319	1.376	1.961	2.050	[187]
[Fe(DFOE)]	1.275	1.307	1.381	1.959	2.055	[188]
[Fe(retro-DFOE)]	1.274	1.321	1.380	1.982	2.043	[189]
[Fe(isotriornicin)]	1.31	1.32	1.37	1.99	2.03	[190]
Average (n = 8)	1.280(12)	1.316(7)	1.378(6)	1.976(11)	2.041(9)	
Average (n = 6)[b]	1.272(4)	1.311(14)	1.377(7)	1.973(11)	2.052(6)	
[Pu(DFOE)(H$_2$O)$_3$]$^+$[c]	1.239	1.331	1.392	2.305	2.362	[109]

[a] Ligand abbreviations: DFC = desferrichrome; DFCA = desferrichrome A; DFOD$_1$ = desferrioxamine D$_1$; DFOE = desferrioxamine E (Scheme 3; **8**).
[b] Fe(III)–tris-monohydroxamato complexes from Table 2.
[c] Pu(VI)–OH$_2$ average bond lengths = 2.463 Å.

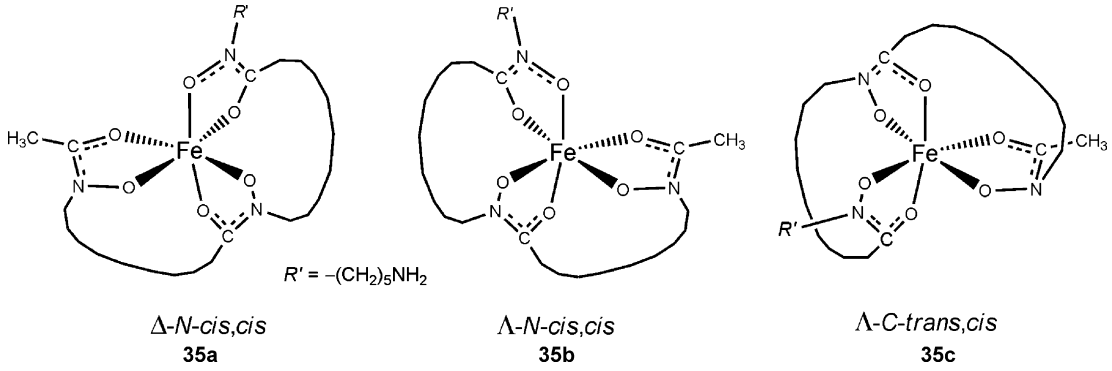

Fig. 12. Optical and geometric isomers of ferrioxamine B (FOB) determined by X-ray crystallography in the absence (**35a**, **35b**) [185] and presence (**35c**) of the cognate FOB-binding protein, FhuD [191].

interaction between FOB and FhuD is enantioselective and also exhibits geometric selectivity. The preferred geometrical isomer of FOB as the binary FOB–FhuD complex, relative to free FOB, could be influenced by the orientation of the amine tail of FOB in the FhuD binding pocket.

The interaction between Λ-*C-trans*, *cis*-FOB and FhuB reveal polyvalent hydrogen bonding interactions between the guanidinium head group of Arg84 and the three hydroxamato oxygen atoms (O2, O3 and O6: atom numbering as per the single molecule of FOB [185]). There is also a hydrogen bonding interaction between Tyr106 and O1 and an interaction between Asp61 and a water molecule and the carbonyl oxygen atom (O7) on the C1-N2 ring. The Λ-*C-trans*, *cis*-FOB isomer sits in the FhuD protein pocket bound by the hydrophobic residues, Trp43, Trp68, Trp273 and Tyr275. If the enantiomer of Λ-*C-trans*, *cis*-FOB is docked into the Fe(III)-siderophore binding pocket, the hydrogen bonding network between Arg84 and O2, O3 and O6 is disrupted (Fig. 13). A monovalent hydrogen bond interaction occurs between Arg84 and O4 in the FhuD-Δ-*C-trans*, *cis*-FOB complex. Further, there is an unfavorable steric clash between the DFO terminal methyl group (C25) and Arg84 in addition to the loss of the interaction between Asp61 and the carbonyl oxygen group. There are no apparent steric clashes in terms of the hydrophobic residues which line the pocket. Therefore, it appears that the enantioselectivity of FOB–FhuD binding is directed by altered hydrogen-bonding networks, rather than steric clashes alone.

The X-ray crystal structure of gallichrome (apoferrichrome ((Gly)$_3$-(*N*-δ-acetyl-*N*-δ-hydroxy-L-ornithine)$_3$) metallated with Ga(III)) bound to the periplasmic binding protein FhuD from *E. coli* has been solved to 1.9 Å resolution [192]. The Ga(III)–O bond lengths in gallichrome range between 2.15 Å and 2.28 Å, which are 0.1 Å longer than in gallichrome in the absence of the cognate binding protein [186]. The strength of conclusions drawn in relation to the metal-O bond lengths is tempered somewhat by the limits of the resolution of the protein crystal structures. It is surprising that although the ferrichrome–FhuD binding constant is 0.1 μM [193], only 45% of gallichrome is buried in the complex. The interaction between Arg84 and two carbonyl oxygen atoms of the hydroxamato moiety are thought to be essential to the complex formation, in addition to the third carbonyl oxygen atom and Tyr 106. The X-ray crystal structure of ferrichrome bound to FhuA from *E. coli* (2.7 Å resolution) shows a significant conformational change in FhuA upon binding ferrichrome in a tyrosine-rich binding pocket [194]. As distinct from the FOB–FhuD system, the conformation of ferrichrome in the binary ferrichrome–FhuA complex is not changed significantly from the conformation of free ferrichrome [186].

The outer membrane transport proteins which recognize Fe(III)-loaded polyhydroxamato complexes are generally found to have 22-stranded antiparallel β-barrel type structures with a β-sheet NH_2-terminal cork domain and a series of short α-helices in the barrel interior [194–197]. The Fe(III)–siderophore complexes, including albomycin [196], ferricrocin [197] or ferrichrome [194] are bound to the FhuA receptor by a network of hydrogen bonds or van der Waals contacts with residues from the cork and barrel domains as shown for the complex between the antibiotic albomycin and FhuA from *E. coli* [196] (Fig. 14).

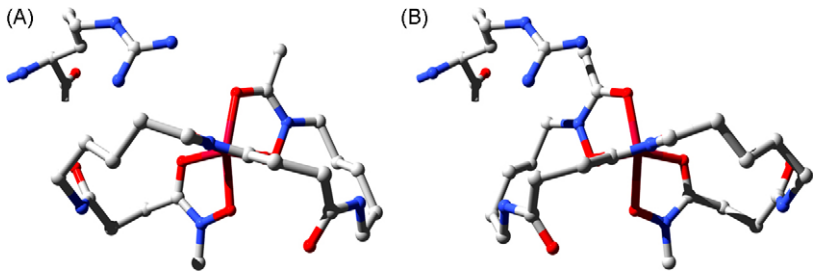

Fig. 13. X-ray crystal structure (2.0 Å resolution) of Λ-*C-trans*, *cis*-FOB (A) or the superposed enantiomer (Δ-*C-trans*, *cis*-FOB) (B) complexed with the periplasmic transport protein FhuD. Figure generated using Swiss-PdbViewer v3.7 [175] and POV-Ray v3.6 [176].

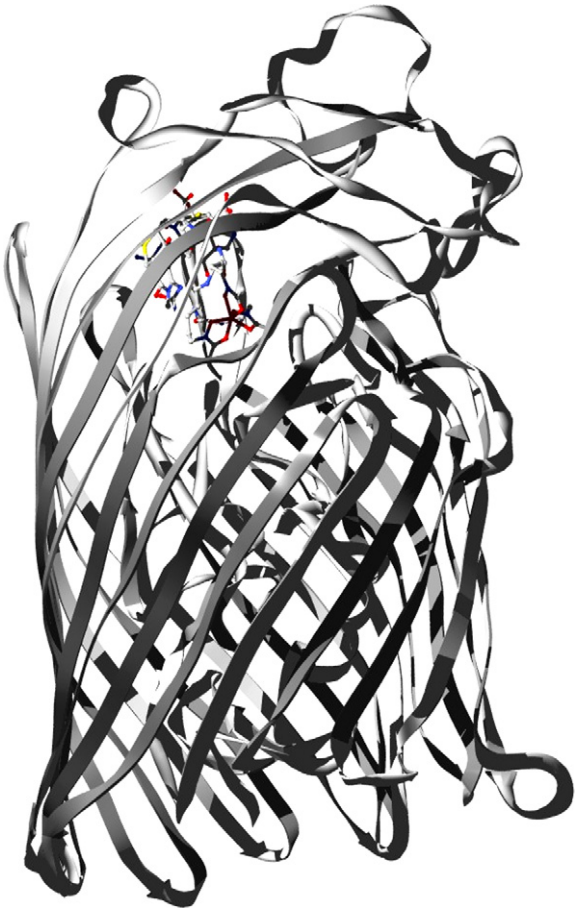

Fig. 14. Albomycin complexed with the outer membrane transporter FhuA from *Escherichia coli* [196].

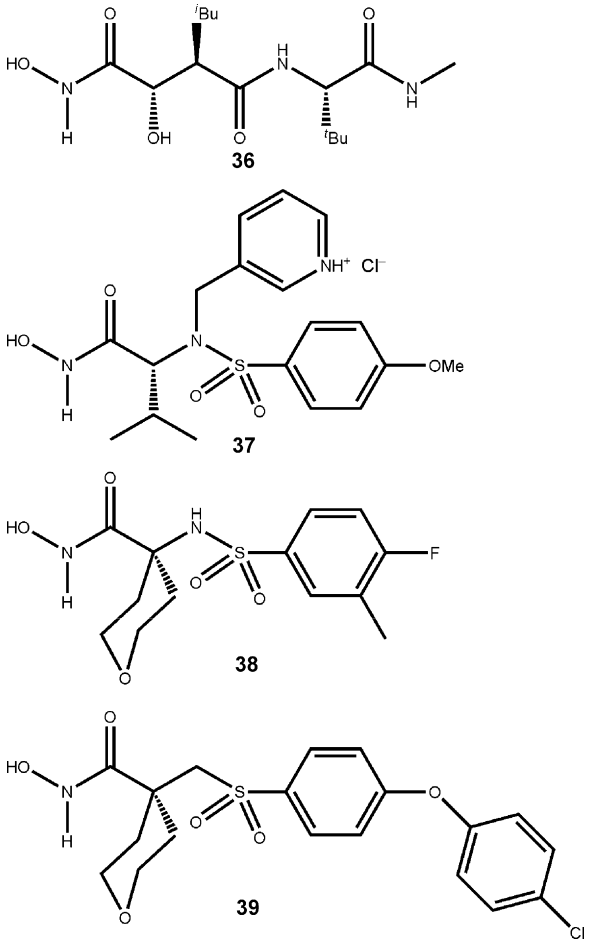

Fig. 15. Marimastat (**36**) and hydroxamic acid–sulfone compounds (**37–39**) that inhibit Zn(II)-containing MMPs.

5. Hydroxamic acids in medicine

The key roles that hydroxamic acid-containing siderophores play in medicine are in the treatment of iron-overload disease and as potential inhibitors of matrix metalloproteinases, selected carbonic anhydrase isoenzymes and the tumor necrosis factor-α converting enzyme (TACE) [198,199]. These roles arise from the metal chelating ability of the hydroxamato/imato functionality. The pharmacological potential of hydroxamic acids has been reviewed recently [200,201].

The most significant use of hydroxamic acids in medicine is the current use of the mesylate salt of DFOB (Desferal®) for the treatment of iron-overload disease in humans. Desferrioxamine B is produced by the soil bacterium, *Streptomyces pilosus* [202]. Iron overload occurs in humans as a consequence of undergoing frequent blood transfusions necessary for the treatment of primary blood disorders such as β-thalassemia. Iron overload leads to serious complications including organ failure and is a major contributor to the mortality rate associated with β-thalassemia. While DFOB is an effective Fe(III) (and Al(III)) chelate in humans, it is not orally active and must be administered to patients subcutaneously [15,203,204]. In some cases, the treatment regime is intolerable to patients; in the absence of iron chelation therapy, the accumulation of iron will ultimately prove fatal. The shortcomings of the use of Desferal® in the clinic in terms of patient compliance fuels research into alternative naturally occurring hydroxamic acid-containing molecules and also in the search for synthetic organic Fe(III) chelates [14,205,206]. In the last decade, two new iron-chelating drugs have appeared: deferiprone (1,2-dimethyl-3-hydroxy-4-pyridone) and deferasirox (4-[3,5-bis(2-hydroxyphenyl)-1,2,4-triazol-1-yl]benzoic acid: ICL 670); while orally available, the use of deferiprone or deferasirox can incur undesirable side effects, such as arthralgias [203]. At the present time, deferasirox is in Phase III of clinical trials for patients with transfusion-dependent anemia and has been granted orphan drug status in the European Union [207]. Desferrioxamine and deferiprone are also being used in combination therapy [208].

The use of hydroxamic acids as inhibitors of MMPs and tumor necrosis factor-α converting enzyme (TACE) is attracting considerable research [199,209]. The catalytic product of the Zn(II)-containing TACE, tumor necrosis factor-α (TNFα), has been implicated in several diseases which include rheumatoid arthritis, Crohn's disease and multiple sclerosis [199]. A suite of sulfonamide and sulfone hydroxamic acid TACE inhibitors have shown promise in the ability to decrease the release of pro-inflammatory cytokines [210]. Modifications of the lead compound, marimastat (Fig. 15; **36**), which was shown to have MMP-inhibition properties has lead to the

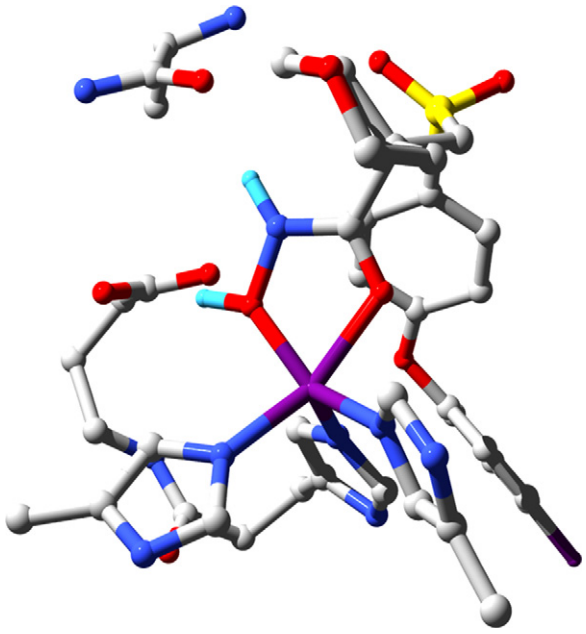

Fig. 16. The diphenylether sulfone, RS-130830, bound to the Zn(II) active site of human collagenase-3 (MMP-13) [21]. Figure generated using Swiss-PdbViewer v3.7 [175] and POV-Ray v3.6 [176]. Hydrogen atoms have been omitted for clarity, excluding the two in the hydroxamic acid chelate (N(H)—O(H)) that are involved in hydrogen-bonding interactions with Ala186 or Glu223, respectively.

development of many compounds that inhibit Zn(II)-dependent metalloproteases [201]. In addition to hydroxamic acids, an array of alternative ZBG are known, including primary sulfonamides (RSO_2NH_2), sulfamates ($ROSO_2NH_2$) and sulfamides ($RNHSO_2NH_2$) [200,209,211,212]. The most promising lead candidates are sulfonated amino acid hydroxamic acids, such as CGS 27023A (**37**) which was found to inhibit stromelysin (MMP-3) [213]. While the primary sulfonamide group is a better ZBG that the hydroxamic acid moiety, the selectivity of the drug candidate toward carbonic anhydrase I (cytosolic isozyme), carbonic anhydrase II (cytosolic) and carbonic anhydrase IX (transmembrane, tumor-associated) is directed by the presence of the hydroxamic acid motif [214]. The compound **38** has been shown to inhibit the lethal factor (LF), a Zn(II)-dependent metalloprotease of the anthrax toxin [215]. Mixed-ligand Fe(III) complexes with marimastat or $ahaH_2$ or $bhaH_2$ have recently been characterized [216] in addition to $[Co(tpa)(mmst)]ClO_4{\cdot}4H_2O$ (mmst = marimasat(2−)) [116] as models for hypoxia activated drug carriers. Derivatives of *o*-aminobenzohydroxamic acid (anthranilic acid) have been found to inhibit prostaglandin H_2 synthase peroxidase activity [217], which is relevant to modulating the inflammation cascade.

The X-ray crystal structure of human collagenase-3 (MMP-13) bound with the inhibitor RS-130830 (Fig. 15, **39**) shows a hydrogen-bond interaction between the N(H)O of the hydroxamic acid group and the amide O atom from the alanine (Ala186) (Fig. 16) [21]. The second hydrogen bond interaction is between the NHOH and the carboxylate head group of Glu223. The hydroxamic acid binding mode is of the type in **32a**. This molecule shows a selectivity towards inhibition of MMP-13 ($K_i = 0.52$ nM) that is 1.135 times the inhibition shown toward MMP-1 ($K_i = 590$ nM) [21]. The selectivity has been attributed to the fit of the diphenylether sulfone group into the MMP S1′ pockets of MMP-1 and MMP-13 which differ in size and shape.

6. Conclusions and frontiers

The richness of the coordination chemistry of hydroxamic acids stems from the wide range of transition metal ions and the diverse coordination modes of the many complexes that have been characterized by X-ray crystallography and in solution. Hydroxamic acids are in the spotlight in chemical biology as ligands at the active sites of Ni(II)- or Zn(II)-containing metalloproteins and as key functional groups of siderophores biosynthesized by bacteria. The ongoing use of a naturally derived trihydroxamic acid siderophore in human medicine further illustrates the extent to which these ligands traverse coordination chemistry, chemical biology and medical science.

Studies of hydroxamic acids continue to reveal potential uses in heavy metal extraction procedures [218] and nuclear fuel reprocessing [219], in materials chemistry and in biomedical applications. Results from studies of the photophysical properties of Fe(III) or Ga(III) complexes with a pyrene-tethered hydroxamic acid ligand have implications in the development of supramolecular switching devices [220]. Hydroxamic acids have also been used in the self-assembly of gold-tethered metal–organic multilayers which enables a high level of control over the molecular architecture of the material [221]. Furthermore, a trihydroxamic acid ligand has been appended to a 7-amino acid peptide fragment designed to target gastrin-releasing peptide receptors as a delivery agent for radioactive Re-188 [222]. The use of hydroxamic acids as affinity probes in proteomics applications is also a growing area of interest [223,224]. Clearly, the applications and fascination of hydroxamic acids have not yet been exhausted.

Acknowledgements

Support from a University of Sydney Bridging Support Grant (2007), the Hermon Slade Foundation and the Australian Antarctic Division (Australian Antarctic Science Grant; Project No. 2547) is gratefully acknowledged.

References

[1] S. Abbasi, Anal. Chem. 48 (1976) 714.
[2] B. Kurzak, H. Kozlowski, E. Farkas, Coord. Chem. Rev. 114 (1992) 169.
[3] J.B. Neilands, J. Biol. Chem. 270 (1995) 26723.
[4] J.M.I. Roosenberg, Y.-M. Lin, Y. Lu, M.J. Miller, Curr. Med. Chem. 7 (2000) 159.
[5] H. Drechsel, G. Jung, J. Peptide Sci. 4 (1998) 147.
[6] A. Butler, BioMetals 18 (2005) 369.
[7] S.M. Kraemer, A. Butler, P. Borer, J. Cervini-Silva, Rev. Mineral. Geochem. 59 (2005) 53.
[8] A.-M. Albrecht-Gary, A.L. Crumbliss, in: A. Sigel, H. Sigel (Eds.), Metal Ions in Biological Systems, vol. 35, Marcel Dekker, Inc., New York, 1998, p. 239.
[9] H. Drechsel, G. Winkelmann, in: G. Winkelmann, C.J. Carrano (Eds.), Transition Metals in Microbial Metabolism, Harwood Academic, Amsterdam, 1997, p. 1.

[10] E.A. Dertz, K.N. Raymond, in: J.A. McCleverty, T.J. Meyer (Eds.), Comprehensive Coordination Chemistry II, vol. 8, Elsevier Pergamon, Boston, 2004, p. 141.
[11] A. Stintzi, K.N. Raymond, in: D.M. Templeton (Ed.), Molecular and Cellular Iron Transport, Marcel Dekker, Inc., New York, 2002, p. 273.
[12] K.N. Raymond, E.A. Dertz, in: J.H. Crosa, A.R. Mey, S.M. Payne (Eds.), Iron Transport in Bacteria, ASM Press, Washington, DC, 2004, p. 3.
[13] J. Faraldo-Gómez, M.S.P. Sansom, Nat. Rev. Mol. Cell. Biol. 4 (2003) 105.
[14] D.S. Kalinowski, D.R. Richardson, Pharmacol. Rev. 57 (2005) 547.
[15] T.B. Chaston, D.R. Richardson, Am. J. Hematol. 73 (2003) 200.
[16] S. Benini, W.R. Rypniewski, K.S. Wilson, S. Miletti, S. Ciurli, S. Mangani, J. Biol. Inorg. Chem. 5 (2000) 110.
[17] L.R. Scolnick, A.M. Clements, J. Liao, L. Crenshaw, M. Hellberg, J. May, T.R. Dean, D.W. Christianson, J. Am. Chem. Soc. 119 (1997) 850.
[18] I. Bertini, V. Calderone, M. Cosenza, M. Fragai, Y.-M. Lee, C. Luchinat, S. Mangani, B. Terni, P. Turano, Proc. Acad. Natl. Sci. U.S.A. 102 (2005) 5334.
[19] H. Nar, K. Werle, M.M. Bauer, H. Dollinger, B. Jung, J. Mol. Biol. 312 (2001) 743.
[20] H. Brandstetter, R.A. Engh, E.G. Von Roedern, L. Moroder, R. Huber, W. Bode, F. Grams, Protein Sci. 7 (1998) 1303.
[21] B. Lovejoy, A.R. Welch, S. Carr, C. Luong, C. Broka, R.T. Hendricks, J.A. Campbell, K.A. Walker, R. Martin, H. Van Wart, M.F. Browner, Nat. Struct. Biol. 6 (1999) 217.
[22] I. Bertini, V. Calderone, M. Fragai, C. Luchinat, S. Mangani, B. Terni, J. Mol. Biol. 336 (2004) 707.
[23] M.G. Natchus, R.G. Bookland, B. De, N.G. Almstead, S. Pikul, M.J. Janusz, S.A. Heitmeyer, E.B. Hookfin, L.C. Hsieh, M.E. Dowty, C.R. Dietsch, V.S. Patel, S.M. Garver, F. Gu, M.E. Pokross, G.E. Mieling, T.R. Baker, D.J. Foltz, S.X. Peng, D.M. Bornes, M.J. Strojnowski, Y.O. Taiwo, J. Med. Chem. 43 (2000) 4948.
[24] D.T. Puerta, S.M. Cohen, Inorg. Chem. 41 (2002) 5075.
[25] D.T. Puerta, M.O. Griffin, J.A. Lewis, D. Romero-Perez, R. Garcia, F.J. Villarreal, S.M. Cohen, J. Biol. Inorg. Chem. 11 (2006) 131.
[26] B. Chatterjee, Coord. Chem. Rev. 26 (1978) 281.
[27] K. Yang, B. Lou, Mini-Rev. Med. Chem. 3 (2003) 349.
[28] C.R. Hauser, W.B.J. Renfrow, in: A.H. Blatt (Ed.), Organic Syntheses, vol. 2, John Wiley & Sons, New York, 1943, p. 67.
[29] W.B.J. Renfrow, C.R. Hauser, J. Am. Chem. Soc. 59 (1937) 2308.
[30] A.S. Reddy, Kumar, G.R. Reddy, Tetrahedron Lett. 41 (2000) 6285.
[31] M.L. Bade, J. Am. Chem. Soc. 93 (1971) 949.
[32] M.P. Sibi, H. Hasegawa, S.R. Ghorpade, Org. Lett. 4 (2002) 3343.
[33] G. Giacomelli, A. Porcheddu, M. Salaris, Org. Lett. 5 (2003) 2715.
[34] M.A. Bailén, R. Chinchilla, D.J. Dodsworth, C. Nájera, Tetrahedron Lett. 42 (2001) 5013.
[35] Z. Yin, K. Low, P. Lye, Synth. Commun. 35 (2005) 2945.
[36] A. Porcheddu, G. Giacomelli, J. Org. Chem. 71 (2006) 7057.
[37] L.A. Watanabe, B. Jose, T. Kato, N. Nishino, M. Yoshida, Tetrahedron Lett. 45 (2004) 491.
[38] A. Volonterio, S. Bellosta, P. Bravo, M. Canavesi, E. Corradi, S.V. Meille, M. Monetti, N. Moussier, M. Zanda, Eur. J. Org. Chem. (2002) 428.
[39] S. Price, S.E. Osbourn, Org. Lett. 7 (2005) 3761.
[40] A.E. Fazary, J. Chem. Eng. Data 50 (2005) 888.
[41] O.N. Ventura, J.B. Rama, L. Turi, J.J. Dannenberg, J. Am. Chem. Soc. 115 (1993) 5754.
[42] F.G. Bordwell, H.E. Fried, D.L. Hughes, T.-Y. Lynch, A.V. Satish, Y.E. Whang, J. Org. Chem. 55 (1990) 3330.
[43] D.C. Edwards, S.C.B. Myneni, J. Phys. Chem. A 110 (2006) 11809.
[44] R. Kakkar, R. Grover, P. Chadha, Org. Biomol. Chem. 1 (2003) 2200.
[45] D.-H. Wu, J.-J. Ho, J. Phys. Chem. A 102 (1998) 3582.
[46] R. Kakkar, R. Grover, P. Gahlot, Polyhedron 25 (2006) 759.
[47] R. Kakkar, R. Grover, P. Gahlot, Theochemistry 767 (2006) 175.
[48] D.C. Edwards, S.C.B. Myneni, J. Phys. Chem. A 109 (2005) 10249.
[49] B.H. Bracher, R.W.H. Small, Acta Crystallogr. B 26 (1970) 1705.
[50] I.K. Larsen, Acta Crystallogr. B 44 (1988) 527.
[51] R.R. Mocherla, D.R. Powell, C.L. Barnes, D. van der Helm, Acta Crystallogr. C 39 (1983) 868.
[52] R. Mocharla, D.R. Powell, D. van der Helm, Acta Crystallogr. C 40 (1984) 1369.
[53] A. Dietrich, D.R. Powell, D.L. Eng-Wilmot, M.B. Hossain, D. van der Helm, Acta Crystallogr. C 46 (1990) 816.
[54] B. García, S. Gonzalez, F.J. Hoyuelos, S. Ibeas, J.M. Leal, M.L. Senent, T. Biver, F. Secco, M. Venturini, Inorg. Chem. 46 (2007) 3680.
[55] J. Schraml, M. Kvícalová, V. Blechta, L. Soukupová, O. Exner, H.-M. Boldhaus, F. Erdt, C. Bliefert, Magn. Reson. Chem. 38 (2000) 795.
[56] N. Mora-Diez, M.L. Senent, B. Garciá, Chem. Phys. 324 (2006) 350.
[57] M.L. Senent, A. Nino, C.M. Caro, S. Ibeas, B. Garcia, J.M. Leal, F. Secco, M. Venturini, J. Org. Chem. 68 (2003) 6535.
[58] B. García, S. Ibeas, A. Munos, J.M. Leal, C. Ghinami, F. Secco, M. Venturini, Inorg. Chem. 42 (2003) 5434.
[59] D.A. Brown, W.K. Glass, R. Mageswaran, S.A. Mohanmmed, Magn. Reson. Chem. 29 (1991) 40.
[60] C.P. Brink, A.L. Crumbliss, Inorg. Chem. 23 (1984) 4708.
[61] B. Monzyk, A.L. Crumbliss, J. Am. Chem. Soc. 101 (1979) 6203.
[62] J. Podlaha, I. Cisarova, L. Soukupova, J. Schraml, Collect. Czech. Chem. Commun. 65 (2000) 1273.
[63] S. Göttlicher, H. Paulus, Chem. Berl. 115 (1982) 393.
[64] I.K. Larsen, Acta Crystallogr. B 34 (1978) 962.
[65] E.E. Saad, Y. Farina, B.M. Yamin, Acta Crystallogr. E 59 (2003) 1004.
[66] F. Barona-Gomez, U. Wong, A.E. Giannakopulos, P.J. Derrick, G.L. Challis, J. Am. Chem. Soc. 126 (2004) 16282.
[67] S.D. Bentley, K.F. Chater, A.-M. Cerdeño-Tárraga, G.L. Challis, N.R. Thomson, K.D. James, D.E. Harris, M.A. Quail, H. Kieser, D. Harper, A. Bateman, S. Brown, G. Chandra, C.W. Chen, M. Collins, A. Cronin, A. Fraser, A. Goble, J. Hidalgo, T. Hornsby, S. Howarth, C.-H. Huang, T. Kieser, L. Larke, L. Murphy, K. Oliver, S. O'Neil, E. Rabbinowitsch, M.-A. Rajandream, K. Rutherford, S. Rutter, K. Seeger, D. Saunders, S. Sharp, R. Squares, S. Squares, K. Taylor, T. Warren, A. Wietzorrek, J. Woodward, B.G. Barrell, J. Parkhill, D.A. Hopwood, Nature 417 (2002) 141.
[68] G.L. Challis, ChemBioChem 6 (2005) 601.
[69] R.J. Bergeron, J.S. McManis, Tetrahedron 46 (1990) 5881.
[70] K. Shimizu, M. Akiyama, J. Chem. Soc., Chem. Commun. (1985) 183.
[71] R.K. Olsen, K. Ramasamy, J. Org. Chem. 50 (1985) 2264.
[72] R.J. Bergeron, J.S. McManis, P.T. Perumal, S.E. Algee, J. Org. Chem. 56 (1991) 5560.
[73] R.J. Bergeron, J.S. McManis, Tetrahedron 45 (1989) 4939.
[74] P.J. Maurer, M.J. Miller, J. Am. Chem. Soc. 104 (1982) 3096.
[75] J.M. Roosenberg II, M.J. Miller, J. Org. Chem. 65 (2000) 4833.
[76] L. Dong, J.M. Roosenberg, M.J. Miller, J. Am. Chem. Soc. 124 (2002) 15001.
[77] H.J. Lindner, S. Göttlicher, Acta Crystallogr. B 25 (1969) 832.
[78] T.W. Failes, T.W. Hambley, Aust. J. Chem. 53 (2000) 879.
[79] C.J. Marmion, T. Murphy, Z. Starikova, K.B. Nolan, Acta Crystallogr. C 56 (2000) E491.
[80] K. Abu-Dari, K.N. Raymond, J. Am. Chem. Soc. 99 (1977) 2003.
[81] J.L. Brumaghim, K.N. Raymond, J. Am. Chem. Soc. 125 (2003) 12066.
[82] A.T. de Figueiredo, V.M. Deflon, K.E. Bessler, C. Maichle-Mossmer, U. Abram, Polyhedron 21 (2002) 2351.
[83] K. Abu-Dari, K.N. Raymond, Inorg. Chem. 19 (1980) 2034.
[84] K. Abu-Dari, S.J. Barclay, P.E. Riley, K.N. Raymond, Inorg. Chem. 22 (1983) 3085.
[85] A. Biller, C. Burschka, M. Penka, R. Tacke, Inorg. Chem. 41 (2002) 3901.
[86] K. Abu-Dari, J.D. Ekstrand, D.P. Freyberg, K.N. Raymond, Inorg. Chem. 18 (1979) 108.
[87] A. Dietrich, K.A. Fidelis, D.R. Powell, D. van Der Helm, D.L. Eng-Wilmot, J. Chem. Soc., Dalton Trans. (1991) 231.
[88] R.G. Baughman, D.J. Brink, J.M. Butler, P.R. New, Acta Crystallogr. C 56 (2000) 528.
[89] B.A. Borgias, S.J. Barclay, K.N. Raymond, J. Coord. Chem. 15 (1986) 109.
[90] C.A. Matsuba, S.J. Rettig, C. Orvig, Can. J. Chem. 66 (1988) 1809.
[91] D. Tranqui, J. Laugier, P. Boyer, P. Vulliet, Acta Crystallogr. B 34 (1978) 767.
[92] W.L. Smith, K.N. Raymond, J. Am. Chem. Soc. 103 (1981) 3341.

[93] D.C. Fisher, S.J. Barclay-Peet, C.A. Balfe, K.N. Raymond, Inorg. Chem. 28 (1989) 4399.
[94] W. Chen, S. Gao, S.-X. Liu, Acta Crystallogr. C 55 (1999) 531.
[95] C.R. Cornman, G.J. Colpas, J.D. Hoeschele, J. Kampf, V.L. Pecoraro, J. Am. Chem. Soc. 114 (1992) 9925.
[96] S. Gao, J.W. Liu, L.H. Huo, H. Zhao, Acta Crystallogr. E 60 (2004) m1722.
[97] G.A. Brewer, E. Sinn, Inorg. Chem. 20 (1981) 1823.
[98] D.A. Brown, H. Bögge, R. Coogan, D. Doocey, T.J. Kemp, A. Müller, B. Neumann, Inorg. Chem. 35 (1996) 1674.
[99] E. Farkas, H. Csóka, G.S. Bell, D.A. Brown, L.P. Cuffe, N.J. Fitzpatrick, W.K. Glass, W. Errington, T.J. Kemp, J. Chem. Soc., Dalton Trans. (1999) 2789.
[100] S.P. Lin, M.A. Khan, K.M. Nicholas, J. Chem. Soc., Chem. Commun. (1994) 2425.
[101] K. Wieghardt, W. Holzbach, E. Hofer, J. Weiss, Inorg. Chem. 20 (1981) 343.
[102] A. Das, F. Basuli, S.-M. Peng, S. Bhattacharya, Inorg. Chem. 41 (2002) 440.
[103] Q. Li, M.F.C. Guedes Da Silva, A.J.L. Pombeiro, Chem. Eur. J. 10 (2004) 1456.
[104] P. Zheng, M. Cui, Y. Gu, X. Jin, Acta Chim. Sin. 43 (1985) 389.
[105] R. Tacke, R. Bertermann, A. Biller, O. Dannappel, M. Penka, M. Pulm, R. Willeke, Z. Anorg. Allg. Chem. 626 (2000) 1159.
[106] U. Casellato, P.A. Vigato, S. Tamburini, R. Graziani, M. Vidali, Inorg. Chim. Acta 81 (1984) 47.
[107] M.M. Makowska-Grzyska, E. Szajna, C. Shipley, A.M. Arif, M.H. Mitchell, J.A. Halfen, L.M. Berreau, Inorg. Chem. 42 (2003) 7472.
[108] J. Comiskey, E. Farkas, K.A. Krot-Lacina, R.G. Pritchard, C.A. McAuliffe, K.B. Nolan, Dalton Trans. (2003) 4243.
[109] M.P. Neu, J.H. Matonic, C.E. Ruggiero, B.L. Scott, Angew. Chem. Int. Ed. 39 (2000) 1442.
[110] B. Haymore, J.C. Huffman, A. Dobson, S.D. Robinson, Inorg. Chim. Acta 65 (1982) L231.
[111] C.J. Marmion, T. Murphy, K.B. Nolan, J.R. Docherty, Chem. Commun. (2000) 1153.
[112] A. Das, F. Basuli, L.R. Falvello, S. Bhattacharya, Inorg. Chem. 40 (2001) 4085.
[113] S.K. Maiti, K.M.A. Malik, S. Gupta, S. Chakraborty, A.K. Ganguli, A.K. Mukherjee, R. Bhattacharyya, Inorg. Chem. 45 (2006) 9843.
[114] M. Haratake, M. Fukunaga, M. Ono, M. Nakayama, J. Biol. Inorg. Chem. 10 (2005) 250.
[115] T.W. Failes, T.W. Hambley, Dalton Trans. (2006) 1895.
[116] T.W. Failes, C. Cullinane, C.I. Diakos, N. Yamamoto, J.G. Lyons, T.W. Hambley, Chem. Eur. J. 13 (2007) 2974.
[117] M. Dolores Santana, G. García, J. Pérez, E. Molins, G. López, Inorg. Chem. 40 (2001) 5701.
[118] K. Rudzka, M.M. Makowska-Grzyska, E. Szajna, A.M. Arif, L.M. Berreau, Chem. Commun. (2005) 489.
[119] T.J. King, P.G. Harrison, J. Chem. Soc., Chemical Commun. (1972) 815.
[120] M.D. Hall, T.W. Failes, D.E. Hibbs, T.W. Hambley, Inorg. Chem. 41 (2002) 1223.
[121] T.W. Failes, T.W. Hambley, Aust. J. Chem. 56 (2003) 45.
[122] R.D. Shannon, Acta Crystallogr. A 32 (1976).
[123] A.J. Stemmler, J.W. Kampf, M.L. Kirk, V.L. Pecoraro, J. Am. Chem. Soc. 117 (1995) 6368.
[124] M. Arnold, D.A. Brown, O. Deeg, W. Errington, W. Haase, K. Herlihy, T.J. Kemp, H. Nimir, R. Werner, Inorg. Chem. 37 (1998) 2920.
[125] D.A. Brown, W. Errington, W.K. Glass, W. Haase, T.J. Kemp, H. Nimir, S.M. Ostrovsky, R. Werner, Inorg. Chem. 40 (2001) 5962.
[126] D.A. Brown, W. Errington, N.J. Fitzpatrick, W.K. Glass, T.J. Kemp, H. Nimir, A.T. Ryan, Chem. Commun. (2002) 1210.
[127] B. Chevrier, H. D'Orchymont, C. Schalk, C. Tarnus, D. Moras, Eur. J. Biochem. 237 (1996) 393.
[128] D.A. Brown, G.J. Clarkson, N.J. Fitzpatrick, W.K. Glass, A.J. Hussein, T.J. Kemp, H. Müller-Bunz, Inorg. Chem. Commun. 7 (2004) 495.
[129] D.A. Brown, N.J. Fitzpatrick, H. Müller-Bunz, A.T. Ryan, Inorg. Chem. 45 (2006) 4497.
[130] S.J. Barclay, K.N. Raymond, Inorg. Chem. 25 (1986) 3561.
[131] D. Gaynor, Z.A. Starikova, S. Ostrovsky, W. Haase, K.B. Nolan, Chem. Commun. (2002) 506.
[132] G. Psomas, C. Dendrinou-Samara, M. Alexiou, A. Tsohos, C.P. Raptopoulou, A. Terzis, D.P. Kessissoglou, Inorg. Chem. 37 (1998) 6556.
[133] D. Gaynor, Z.A. Starikova, W. Haase, K.B. Nolan, Dalton Trans. (2001) 1578.
[134] M.S. Lah, V.L. Pecoraro, J. Am. Chem. Soc. 111 (1989) 7258.
[135] S.H. Seda, J. Janczak, J. Lisowski, Inorg. Chem. Commun. 9 (2006) 792.
[136] T.N. Parac-Vogt, A. Pacco, P. Nockemann, Y.-F. Yuan, C. Gorller-Walrand, K. Binnemans, Eur. J. Inorg. Chem. (2006) 1466.
[137] G. Psomas, A.J. Stemmler, C. Dendrinou-Samara, J.J. Bodwin, M. Schneider, M. Alexiou, J.W. Kampf, D.P. Kessissoglou, V.L. Pecoraro, Inorg. Chem. 40 (2001) 1562.
[138] B. Kurzak, E. Farkas, T. Glowiak, H. Kozlowski, J. Chem. Soc., Dalton Trans. (1991) 163.
[139] S. Trofimenko, Chem. Rev. 93 (1993) 943.
[140] A.D. Cutland, J.A. Halfen, J.W. Kampf, V.L. Pecoraro, J. Am. Chem. Soc. 123 (2001) 6211.
[141] A.D. Cutland-Van Noord, J.W. Kampf, V.L. Pecoraro, Angew. Chem. Int. Ed. 41 (2002) 4667.
[142] A.J. Stemmler, J.W. Kampf, M.L. Kirk, B.H. Atasi, V.L. Pecoraro, Inorg. Chem. 38 (1999) 2807.
[143] A. Pacco, T.N. Parac-Vogt, E. van Besien, K. Pierloot, C. Gorller-Walrand, K. Binnemans, Eur. J. Inorg. Chem. (2005) 3303.
[144] J.J. Bodwin, A.D. Cutland, R.G. Malkani, V.L. Pecoraro, Coord. Chem. Rev. 216–217 (2001) 489.
[145] V.L. Pecoraro, A.J. Stemmler, B.R. Gibney, J.J. Bodwin, H. Wang, J.W. Kampf, A. Barwinski, Prog. Inorg. Chem. 45 (1997) 83.
[146] R.M. Yeh, A.V. Davis, K.N. Raymond, in: J.A. McCleverty, T.J. Meyer (Eds.), Comprehensive Coordination Chemistry II, vol. 7, Elsevier Pergamon, Amsterdam, 2004, p. 327.
[147] J.A. Johnson, J.W. Kampf, V.L. Pecoraro, Angew. Chem. Int. Ed. 42 (2003) 546.
[148] L. Cheng, M.A. Khan, R.W. Taylor, G.B. Richter-Addo, D.R. Powell, Chem. Commun. (1999) 1941.
[149] D.A. Brown, A.L. Roche, T.A. Pakkanen, T.T. Pakkanen, K. Smolander, J. Chem. Soc., Dalton Trans. (1982) 676.
[150] J. Świątek-Kozlowska, E. Gumienna-Kontecka, A. Dobosz, I.A. Golenya, I.O. Fritsky, Dalton Trans. (2002) 4639.
[151] W. Henderson, C. Evans, B.K. Nicholson, J. Fawcett, Dalton Trans. (2003) 2691.
[152] D. Griffith, K. Lyssenko, P. Jensen, P.E. Kruger, C.J. Marmion, Dalton Trans. (2005) 956.
[153] C. Mulcahy, F.M. Dolgushin, K.A. Krot, D. Griffith, C.J. Marmion, Dalton Trans. (2005) 1993.
[154] T.W. Failes, M.D. Hall, T.W. Hambley, Dalton Trans. (2003) 1596.
[155] E. Farkas, H. Csóka, G. Micera, A. Dessi, J. Inorg. Biochem. 65 (1997) 281.
[156] E. Farkas, E. Kozman, M. Petho, K.M. Herlihy, G. Micera, Polyhedron 17 (1998) 3331.
[157] N. Gálvez, B. Ruiz, R. Cuesta, E. Colacio, J.M. Domínguez-Vera, Inorg. Chem. 44 (2005) 2706.
[158] P. Buglyo, N. Potari, Polyhedron 24 (2005) 837.
[159] E. Farkas, E.A. Enyedy, G. Micera, E. Garribba, Polyhedron 19 (2000) 1727.
[160] L. Morroni, F. Secco, M. Venturini, B. Garcia, J.M. Leal, Inorg. Chem. 43 (2004) 3005.
[161] J.H. Bell, R.F. Pratt, Biochemistry 41 (2002) 4329.
[162] S. Gez, R. Luxenhofer, A. Levina, R. Codd, P.A. Lay, Inorg. Chem. 44 (2005) 2934.
[163] E. Farkas, H. Csóka, I. Toth, Dalton Trans. (2003) 1645.
[164] D.A. Brown, R. Geraty, J.D. Glennon, N.N. Choileain, Inorg. Chem. 25 (1986) 3792.
[165] A. Evers, R.D. Hancock, A.E. Martell, R.J. Motekaitis, Inorg. Chem. 28 (1989) 2189.
[166] I. Spasojevic, H. Boukhalfa, R.D. Stevens, A.L. Crumbliss, Inorg. Chem. 40 (2001) 49.

[167] I. Spasojevic, S.K. Armstrong, T.J. Brickman, A.L. Crumbliss, Inorg. Chem. 38 (1999) 449.
[168] Z. Hou, C.J. Sunderland, T. Nishio, K.N. Raymond, J. Am. Chem. Soc. 118 (1996) 5148.
[169] F.C. Kuepper, C.J. Carrano, J.-U. Kuhn, A. Butler, Inorg. Chem. 45 (2006) 6028.
[170] G. Schwarzenbach, K. Schwarzenbach, Helv. Chim. Acta 46 (1963) 1390.
[171] H. Boukhalfa, S.D. Reilly, M.P. Neu, Inorg. Chem. 46 (2007) 1018.
[172] Z. Amtul, Atta-ur-Rahman, R.A. Siddiqui, M.I. Choudhary, Curr. Med. Chem. 9 (2002) 1323.
[173] A.W. Addison, T.N. Rao, J. Reedijk, J. van Rijn, G.C. Verschoor, J. Chem. Soc., Dalton Trans. (1984) 1349.
[174] M.A. Pearson, L.O. Michel, R.P. Hausinger, P.A. Karplus, Biochemistry 36 (1997) 8164.
[175] N. Guex, M.C. Peitsch, Electrophoresis 18 (1997) 2714.
[176] C. Cason, T. Fröhlich, N. Kopp, Persistence of Vision Raytracer (Version 3.6), 2004. Retrieved from http://www.povray.org/.
[177] R. Lang, A. Kocourek, M. Braun, H. Tschesche, R. Huber, W. Bode, K. Maskos, J. Mol. Biol. 312 (2001) 731.
[178] R. Morales, S. Perrier, J.-M. Florent, J. Beltra, S. Dufour, I. De Mendez, P. Manceau, A. Tertre, F. Moreau, D. Compere, A.-C. Dublanchet, M. O'Gara, J. Mol. Biol. 341 (2004) 1063.
[179] W.L. Shoop, Y. Xiong, J. Wiltsie, A. Woods, J. Guo, J.V. Pivnichny, T. Felcetto, B.F. Michael, A. Bansal, R.T. Cummings, B.R. Cunningham, A.M. Friedlander, C.M. Douglas, S.B. Patel, D. Wisniewski, G. Scapin, S.P. Salowe, D.M. Zaller, K.T. Chapman, E.M. Scolnick, D.M. Schmatz, K. Bartizal, M. MacCoss, J.D. Hermes, Proc. Acad. Natl. Sci. U.S.A. 102 (2005) 7958.
[180] B.E. Turk, T.Y. Wong, R. Schwarzenbacher, E.T. Jarrell, S.H. Leppla, R.J. Collier, R.C. Liddington, L.C. Cantley, Nat. Struct. Biol. 11 (2004) 60.
[181] Z. Fu, S. Chen, M.R. Baldwin, G.E. Boldt, A. Crawford, K.D. Janda, J.T. Barbieri, J.-J.P. Kim, Biochemistry 45 (2006) 8903.
[182] A. Vannini, C. Volpari, G. Filocamo, E.C. Casavola, M. Brunetti, D. Renzoni, P. Chakravarty, C. Paolini, R. De Francesco, P. Gallinari, C. Steinkuehler, S. Di Marco, Proc. Acad. Natl. Sci. U.S.A. 101 (2004) 15064.
[183] J.R. Somoza, R.J. Skene, B.A. Katz, C. Mol, J.D. Ho, A.J. Jennings, C. Luong, A. Arvai, J.J. Buggy, E. Chi, J. Tang, B.-C. Sang, E. Verner, R. Wynands, E.M. Leahy, D.R. Dougan, G. Snell, M. Navre, M.W. Knuth, R.V. Swanson, D.E. McRee, L.W. Tari, Structure 12 (2004) 1325.
[184] M.S. Finnin, J.R. Donigian, A. Cohen, V.M. Richon, R.A. Rifkind, P.A. Marks, R. Breslow, N.P. Pavletich, Nature 401 (1999) 188.
[185] S. Dhungana, P.S. White, A.L. Crumbliss, J. Biol. Inorg. Chem. 6 (2001) 810.
[186] D. van der Helm, J.R. Baker, D.L. Eng-Wilmot, M.B. Hossain, R.A. Loghry, J. Am. Chem. Soc. 102 (1980) 4224.
[187] M.B. Hossain, M.A.F. Jalal, D. van der Helm, Acta Crystallogr. C 42 (1986) 1305.
[188] D. van der Helm, M. Poling, J. Am. Chem. Soc. 98 (1976) 82.
[189] M.B. Hossain, M.A.F. Jalal, D. Van Der Helm, K. Shimizu, M. Akiyama, J. Chem. Crystallogr. 28 (1998) 53.
[190] M.B. Hossain, M.A.F. Jalal, B.A. Benson, C.L. Barnes, D. Van der Helm, J. Am. Chem. Soc. 109 (1987) 4948.
[191] T.E. Clarke, V. Braun, G. Winkelmann, L.W. Tari, H.J. Vogel, J. Biol. Chem. 277 (2002) 13966.
[192] T.E. Clarke, S.-Y. Ku, D.R. Dougan, H.J. Vogel, L.W. Tari, Nat. Struct. Biol. 7 (2000) 287.
[193] M.R. Rohrbach, V. Braun, W. Koster, J. Bacteriol. 177 (1995) 7186.
[194] K.P. Locher, B. Rees, R. Koebnik, A. Mitschler, L. Moulinier, J.P. Rosenbusch, D. Moras, Cell 95 (1998) 771.
[195] A.D. Ferguson, W. Welte, E. Hofmann, B. Lindner, O. Holst, J.W. Coulton, K. Diederichs, Structure 8 (2000) 585.
[196] A.D. Ferguson, V. Braun, H.-P. Fiedler, J.W. Coulton, K. Diederichs, W. Welte, Protein Sci. 9 (2000) 956.
[197] A.D. Ferguson, E. Hofmann, J.W. Coulton, K. Diederichs, W. Welte, Science 282 (1998) 2215.
[198] C.J. Marmion, D. Griffith, K.B. Nolan, Eur. J. Inorg. Chem. (2004) 3003.
[199] J.S. Skotnicki, M.J. DiGrandi, J.I. Levin, Curr. Opin. Drug Disc. Dev. 6 (2003) 742.
[200] E.M.F. Muri, M.J. Nieto, R.D. Sindelar, J.S. Williamson, Curr. Med. Chem. 9 (2002) 1631.
[201] B. Lou, K. Yang, Mini-Rev. Med. Chem. 3 (2003) 609.
[202] H. Bickel, G.E. Hall, W. Keller-Schierlein, V. Prelog, E. Vischer, A. Wettstein, Helv. Chim. Acta 43 (1960) 2129.
[203] N.F. Olivieri, G.M. Brittenham, Blood 89 (1997) 739.
[204] L. Merson, N. Olivieri, Blood Rev. 16 (2002) 127.
[205] Z.D. Liu, R.C. Hider, Coord. Chem. Rev. 232 (2002) 151.
[206] G. Faa, G. Crisponi, Coord. Chem. Rev. 184 (1999) 291.
[207] S. Steinhauser, U. Heinz, M. Bartholomä, T. Weyhermüller, H. Nick, K. Hegetschweiler, Eur. J. Inorg. Chem. (2004) 4177.
[208] A. Kattamis, V. Ladis, H. Berdousi, N.L. Kelekis, E. Alexopoulou, I. Papasotiriou, K. Drakaki, I. Kaloumenou, A. Galani, C. Kattamis, Blood Cell. Mol. Dis. 36 (2006) 21.
[209] D.T. Puerta, S.M. Cohen, Curr. Top. Med. Chem. 4 (2004) 1551.
[210] J.I. Levin, J.M. Chen, L.M. Laakso, M. Du, X. Du, A.M. Venkatesan, V. Sandanayaka, A. Zask, J. Xu, W. Xu, Y. Zhang, J.S. Skotnicki, Bioorg. Med. Chem. Lett. 15 (2005) 4345.
[211] S. Chaves, S.M. Marques, A. Cachudo, M.A. Esteves, M.A. Santos, Eur. J. Inorg. Chem. (2006) 3853.
[212] M. Whittaker, C.D. Floyd, P. Brown, A.J.H. Gearing, Chem. Rev. 99 (1999) 2735.
[213] L.J. MacPherson, E.K. Bayburt, M.P. Capparelli, B.J. Carroll, R. Goldstein, M.R. Justice, L. Zhu, S.-i. Hu, R.A. Melton, L. Fryer, R.L. Goldberg, J.R. Doughty, S. Spirito, V. Blancuzzi, D. Wilson, E.M. O'Byrne, V. Ganu, D.T. Parker, J. Med. Chem. 40 (1997) 2525.
[214] M.A. Santos, S. Marques, D. Vullo, A. Innocenti, A. Scozzafava, C.T. Supuran, Bioorg. Med. Chem. Lett. 17 (2007) 1538.
[215] Y. Xiong, J. Wiltsie, A. Woods, J. Guo, J.V. Pivnichny, W. Tang, A. Bansal, R.T. Cummings, B.R. Cunningham, A.M. Friedlander, C.M. Douglas, S.P. Salowe, D.M. Zaller, E.M. Scolnick, D.M. Schmatz, K. Bartizal, J.D. Hermes, M. MacCoss, K.T. Chapman, Bioorg. Med. Chem. Lett. 16 (2006) 964.
[216] T.W. Failes, T.W. Hambley, J. Inorg. Biochem. 101 (2007) 396.
[217] J. Lee, A.J. Chubb, E. Moman, B.M. McLoughlin, C.T. Sharkey, J.G. Kelly, K.B. Nolan, M. Devocelle, D.J. Fitzgerald, Org. Biomol. Chem. 3 (2005) 3678.
[218] J. Szymanowski, M. Wisniewski, Pol. J. Appl. Chem. 40 (1996) 3.
[219] R.J. Taylor, I. May, A.L. Wallwork, I.S. Denniss, N.J. Hill, B.Y. Galkin, B.Y. Zilberman, Y.S. Fedorov, J. Alloys Compd. 271–273 (1998).
[220] B. Bodenant, F. Fages, M.-H. Delville, J. Am. Chem. Soc. 120 (1998) 7511.
[221] A. Hatzor, T. Moav, H. Cohen, S. Matlis, J. Libman, A. Vaskevich, A. Shanzer, I. Rubinstein, J. Am. Chem. Soc. 120 (1998) 13469.
[222] A. Safavy, M.B. Khazaeli, H. Qin, D.J. Buchasbaum, Cancer 80 (1997) 2354.
[223] E.W.S. Chan, S. Chattopadhaya, R.C. Panicker, X. Huang, S.Q. Yao, J. Am. Chem. Soc. 126 (2004) 14435.
[224] J. Wang, M. Uttamchandani, J. Li, M. Hu, S.Q. Yao, Chem. Commun. (2006) 3783.